

THE PENNSYLVANIA STATE UNIVERSITY  
SCHREYER HONORS COLLEGE

DEPARTMENT OF BIOENGINEERING

RE-ENGINEERING BREAST CANCER METABOLISM USING METFORMIN  
AND DICHLOROACETATE

SAMAGYA BANSKOTA  
Spring 2012

A thesis  
submitted in partial fulfillment  
of the requirements  
for a baccalaureate degree  
in Bioengineering  
with honors in Bioengineering

Reviewed and approved\* by the following:

Dr. Anneke Blackburn  
NHMRC R. D. Wright Fellow  
Thesis Supervisor  
The Australian National University

Dr. William Hancock  
Associate Professor of Bioengineering  
Thesis Supervisor  
The Pennsylvania State University

Dr. Peter Butler  
Associate Professor of Bioengineering  
Honors Adviser  
The Pennsylvania State University

\* Signatures are on file in the Schreyer Honors College.

# Abstract

Cancer cells have a unique metabolic phenotype, the Warburg effect which, causes a high rate of glycolysis for ATP generation. This results in increased lactate production and reduced mitochondrial oxidation of pyruvate. This unique metabolic profile is thought to be associated with the resistance of cancer cells to apoptosis. Dichloroacetate(DCA) and metformin are two generic drugs that have recently demonstrated nontoxic anti-neoplastic effect by directly targeting cancer metabolism. DCA is an inhibitor of pyruvate dehydrogenase kinase (PDK), that can reverse the Warburg effect by increasing the flux of pyruvate into the mitochondria while metformin is an anti-diabetic drug that can inhibit proliferation in different types of tumor by targeting complex I of electron transport chain (ETC) and indirectly activating AMP-activated protein kinase (AMPK). The purpose of this study was to characterize the effects of DCA and metformin individually and in combination in an in vitro model of V14 breast cancer cells.

Here, we report that after 72 hours of 5mM DCA and 6mM metformin treatment alone, there were 50% and 60% less viable cells present. When 5mM DCA was combined with metformin, it enhanced metformin's anti-tumor activity at a lower dose, 0.5mM, there was at least 4 fold decrease in viable cell number compared with metformin treatment alone. The robustness of this result was validated by linear regression and measurement error model. DCA and metformin, however did not induce apoptosis, as seen from caspases 3 and 7 activity. The ability of DCA to inhibit PDKs and that of metformin to block complex I of ETC was assessed by measuring extracellular lactate concentration. DCA reduced the extracellular lactate concentration by targeting more pyruvate into the mitochondria, while metformin treated cells compensated for

impaired mitochondrial respiration by increasing glycolysis as seen with increased extracellular lactate concentration. ATP levels also decreased significantly after the combination treatment indicating that there was a severe disruption of energy homeostasis in the cells.

The action of metformin on its targeted molecule, AMPK, was assessed by western blot. Our results demonstrated that metformin activated AMPK in a dose and time dependent manner. Treatment with DCA also activated AMPK. We report a new molecular target of DCA, AMPK. However, the mechanism of AMPK activation by DCA is not fully understood yet but there are strong evidences in the literature that it could be via  $\text{Ca}^{2+}$  signaling.

Together, these data suggest that targeting two aspects of metabolism using dichloroacetate and metformin may be useful in the treatment of cancer.

# Table of Contents

<b>List of Figures</b>	<b>v</b>
<b>List of Tables</b>	<b>vii</b>
<b>Abbreviations</b>	<b>viii</b>
<b>Acknowledgments</b>	<b>ix</b>
<b>Chapter 1</b>	
<b>Introduction</b>	<b>1</b>
1.1 An Overview of Cancer . . . . .	1
1.1.1 The Metabolism of Cancer Cells . . . . .	1
1.2 Role of Warburg effect in carcinogenesis . . . . .	4
1.3 Dichloroacetate (DCA) as an anti-cancer drug . . . . .	5
1.4 Metformin as an anti-cancer drug . . . . .	5
1.4.1 The AMPK pathway . . . . .	7
1.5 Combination treatment of breast cancer with metformin and DCA . . . . .	8
1.5.1 Hypothesis and specific aims . . . . .	10
1.5.1.1 Specific Aims . . . . .	10
<b>Chapter 2</b>	
<b>Materials and Methods</b>	<b>11</b>
2.1 Cell lines and culture conditions . . . . .	11
2.2 Drug treatment . . . . .	11
2.3 Cell proliferation assay . . . . .	12
2.4 Neutral red cell viability assay . . . . .	12
2.5 Analysis of drug interaction . . . . .	13
2.6 Lactate assay . . . . .	13
2.7 Western blotting . . . . .	14
2.8 Cell metabolism . . . . .	15
2.9 Apoptosis assay . . . . .	15
2.10 Statistical analysis . . . . .	15
<b>Chapter 3</b>	
<b>Results</b>	<b>16</b>
3.1 Metformin and DCA treatment in combination is more effective at reducing cell proliferation <i>in vitro</i> . . . . .	16

3.2	Metformin and DCA do not induce apoptosis . . . . .	18
3.3	Metformin and DCA both increase AMPK activity . . . . .	20
3.4	DCA reverses the Warburg effect while metformin inhibits complex I of ETC, disrupting the energy homeostasis . . . . .	23
<b>Chapter 4</b>		
	<b>Discussion</b>	<b>29</b>
4.1	Summary . . . . .	29
4.2	Robustness Analysis . . . . .	32
4.2.1	Ordinary Least Squares . . . . .	33
4.2.2	Robust Regression . . . . .	35
4.2.3	Measurement Error . . . . .	35
4.3	Conclusions . . . . .	41
	<b>Bibliography</b>	<b>42</b>

# List of Figures

1.1	The six hallmarks of cancer cells. [Hanahan & Weinberg, 2000]	2
1.2	Emerging hallmarks and enabling characteristics of cancer cells. [Hanahan & Weinberg, 2011]	2
1.3	Schematic representation of the differences between oxidative phosphorylation, anaerobic glycolysis, and aerobic glycolysis (Warburg Effect). [Image taken from Heiden V, Science 2009]	4
1.4	Remodeling of pyruvate metabolism in cancer cells by treatment with DCA. Modified from (Bonnet et al., 2007).	6
1.5	Targets of metformin and AMPK pathway.	8
1.6	Remodeling of cancer metabolism with metformin and DCA.	9
3.1	Effect of metformin on V14 cells. Images taken by IncuCyte at different time points, 24h, 48h and 72h show that there is reduction in cell number after metformin treatment.	17
3.2	Effect of metformin on V14 cells. The percentages of surviving cells relative to control, defined as 100% survival, were determined by neutral red assay. Data shows the mean of four independent experiments + SEM. ***P < 0.005 versus control.	18
3.3	Effect of DCA on V14 cells. Images taken by IncuCyte at different time points, 24h, 48h and 72h show that there is reduction in cell number after DCA treatment.	19
3.4	Effect of DCA on V14 cells. The percentages of surviving cells relative to control, defined as 100% survival, were determined by neutral red assay. Data shows the mean of four independent experiments + SEM. **P < 0.01 versus control.	20
3.5	Interpolation of IC <sub>50</sub> of DCA and metformin on V14 cell lines after 72 hours exposure. IC <sub>50</sub> is defined as the drug concentration leading to a 50% inhibition of cell growth. Interpolation was done using MATLAB inbuilt function. Data represents the average of four independent experiments.	21
3.6	Evaluation of interaction between DCA and metformin after 72 hours exposure. RI values were calculated from neutral red cell viability assay. Synergism is defined as RI > 1. Values are expressed as mean + SEM, n=4. Significant difference was assessed using t-test, with null hypothesis RI=1.*P < 0.05.	22
3.7	Three dimensional log-log surface plot representing the interaction between DCA and metformin after 72hours exposure.	23
3.8	Metformin and DCA treatment, individually or in combination, did not increase caspase 3 and 7 activity significantly. (A)Caspase 3 and 7 activity after 4 hours of treatment. (B)Caspase 3 and 7 activity after 24 hours of treatment. 1μM Staurosporine is used as a positive control. Values are expressed as mean + SEM, n=3.	24

3.9	Metformin and DCA activates AMPK in a dose-dependent manner. V14 cells were treated with DCA and metformin alone and in combination for 4 hours (A) and 24 hours (B). Phosphorylation of AMPK at (Thr <sup>172</sup> ) was measured by western blot. $\beta$ -Actin is shown as loading control. . . . .	25
3.10	DCA treatment reduced the weight of p53 heterozygous mice. p53 heterozygous mice were put on DCA treatment when they were 4 weeks old until the spontaneous tumor that they developed reached about 1.2 cm in radius. The control group were put on normal water and sacrificed when their spontaneous tumor grew about 1.2 cm in radius. **P< 0.01, ***P< 0.005 versus control. . . . .	26
3.11	Effect of drug treatment on extracellular lactate levels. Relative lactate concentration after 4 hours, 10 hours and 24 hours of DCA treatment. Values are expressed as mean + SEM, n=3. *P<0.05, **P<0.01 versus control. . . . .	26
3.12	Effect of drug treatment on extracellular lactate levels. (A) Relative lactate production after 24 hours of treatment with AICAR and metformin. Values are expressed as mean + SEM, n=3. **P<0.01 versus control. . . . .	27
3.13	Effect of drug treatment on ATP levels. (A) ATP levels after 4 hours of treatment. (B) ATP levels after 24 hours of treatment. Values are expressed as mean + SEM, n=3. *P<0.05, **P<0.01 versus control. . . . .	28
4.1	A model for DCA induced phosphorylation of AMPK. Dichloroacetate results in hypoxia and increased ROS production, which leads to release of Ca <sup>2+</sup> from endoplasmic reticulum(ER) and translocation of STMI (a sensor of calcium stores in ER) to ER domains near the plasma membrane. STMI then activates CRAC (calcium release activated calcium) channels via direct physical interactions with the Orai subunits. This facilitates Ca <sup>2+</sup> influx. Increased cytosolic Ca <sup>2+</sup> activates (CaMKK $\beta$ ), which phosphorylates AMPK. Adapted from Mungai et. al, 2011. .	32
4.2	Variance among the four replicates of raw neutral red data. . . . .	36
4.3	Standard deviation vs. the mean of replicates for raw neutral red data. Each point represents the mean and standard deviation of four replicates in each experiment. The solid line is the predicted relationship between standard deviation and mean of replicates. . . . .	37
4.4	Q-Q plot of composite error and a theoretical normal distribution. The fact that quantiles of the two distributions align along a 45 <sup>0</sup> line indicate that the estimated errors are Gaussian. . . . .	40

# List of Tables

4.1	Summary Statistics . . . . .	34
4.2	Ordinary Least Squares Estimates . . . . .	34
4.3	Robust Regression Estimates . . . . .	35
4.4	Estimated parameters for reading 3 and reading 4 from OLS . . . . .	40
4.5	Estimated parameters for reading 3 and reading 4 from robust regression . . . . .	41
4.6	Corrected estimates for OLS and robust regression . . . . .	41



# Abbreviations

- ACC- acetyl-CoA carboxylase
- AICAR- 5-aminoimidazole-4-carboxamide 1- $\beta$ -D-ribofuranoside
- AIF- apoptosis inducing factor
- AMP- adenosine monophosphate
- AMPK- AMP activated protein kinase
- ATP- adenosine-5'-triphosphate
- CaMKK- calmodulin-dependent protein kinase kinase
- cyt c- cytochrome c
- DCA- dichloroacetate
- ETC- electron transport chain
- IC<sub>50</sub> half maximal inhibitory concentration
- LDH- lactate dehydrogenase
- LKB1- liver kinase B1
- mTOR- mammalian target of rapamycin
- MTP- mitochondrial transition pore
- OLS- ordinary least squares
- pACC- phosphorylated acetyl-CoA carboxylase
- pAMPK- phosphorylated AMPK
- PDH- pyruvate dehydrogenase
- PDK- pyruvate dehydrogenase kinase
- ROS- reactive oxygen species
- TCA- tricarboxylic acid

# Acknowledgments

I am indebted to Dr. Anneke Blackburn, my honors supervisor at the John Curtin School of Medical Research, the Australian National University for giving me the opportunity to visit JCSMR. Without that and her guidance along the way, this thesis would not have seen the light of the day. There are many people both at ANU and Penn State to whom I owe a lot, both intellectually and personally. Among them all, I want to thank Melissa, Bevan, and Santhi for everything they taught me in the past few months. This work was carried out while visiting ANU; their generous hospitality is greatly acknowledged. Molecular Genetics Group in JCSMR provided invaluable support while conducting this research—much thanks.

Funding for this project was partly provided by a grant from Cancer Council, Australia and the Pennsylvania State University's Schreyer Honors College. I also owe a lot, both directly and indirectly to my parents for their relentless support and encouragements.

I would also like to thank my honors advisor, Dr. Peter Butler, for guiding me and advising me in the last few years. In addition, I would like to thank Dr. William Hancock for helping in this thesis and encouraging me to visit ANU.

Lastly, I would like to thank my friend Gaurab, for helping me navigate the labyrinth of Statistical Inference, which was a great resource. Needless to say, all the errors are mine.

# Chapter 1

## Introduction

### 1.1 An Overview of Cancer

Cancer is a general name for a group of more than 100 diseases involving uncontrolled growth of abnormal cells beyond normal tissue boundaries. It is a leading cause of death worldwide. About 571,950 Americans were expected to die of cancer in 2011 i.e. more than 1,500 people a day [1]. Although there are many forms of cancer, the fundamental problems are common across most types and have been described as the six known hallmarks of cancer cells: self-sufficiency in growth signals, insensitivity to growth inhibition, evasion of apoptosis, limitless replicative potential, sustained angiogenesis and invasiveness (Figure 1.1) [2]. Research work done in the last decade has added two more hallmarks: reprogramming of energy metabolism and evading immune destruction (Figure 1.2) [3].

#### 1.1.1 The Metabolism of Cancer Cells

Glucose, a 6-carbon molecule, is converted into pyruvate, a 3-carbon molecule in the cytoplasm of the cells during glycolysis. In normal cells, pyruvate is then transported into the mitochondria where pyruvate oxidation takes place, transforming pyruvate into acetyl-CoA. The enzyme



**Figure 1.1.** The six hallmarks of cancer cells. [Hanahan & Weinberg, 2000]

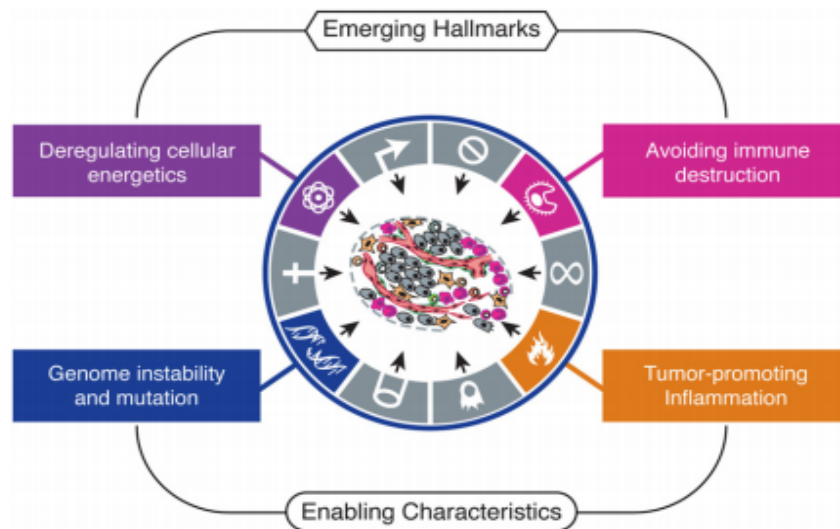


**Figure 1.2.** Emerging hallmarks and enabling characteristics of cancer cells. [Hanahan & Weinberg, 2011]

that controls the process of pyruvate oxidation is called pyruvate dehydrogenase (PDH) [4]. The tricarboxylic acid (TCA) cycle and electron transport chain (ETC) drive the generation of 36-38 ATP molecules per glucose molecule from pyruvate by a process known as oxidative phosphorylation. Briefly, acetyl-CoA enters the inner membrane of mitochondria where it enters the TCA cycle. After the TCA cycle is completed, most of the energy from glucose molecule is transformed into electron carriers, NADH and FADH<sub>2</sub>, which donate the electrons to ETC. This is where ATP synthesis happens. Moreover, NADH produced from the TCA cycle transfers electrons to complex I of the respiratory chain which produces superoxide. Superoxide promotes the opening of the mitochondrial transition pore (MTP) that enables the efflux of cytochrome c (cyt c) and apoptosis inducing factor (AIF) into the cytosol, activating caspases and enhancing apoptosis [5].

However, as described by Otto Warburg in 1931, cancer cells preferentially utilize glycolytic pathways rather than oxidative phosphorylation for energy generation [6]. This metabolic abnormality referred as the 'Warburg effect' in cancer cells is one of the distinctive characteristics that distinguishes them from their normal counterparts.

Glycolysis is the preferred route of energy production in cancer cells under both hypoxic and normoxic conditions. Compared to oxidative phosphorylation, it is an inefficient process of energy generation (releases 2 ATP per glucose molecule), but can operate in an anaerobic condition and produce ATP 100 times faster if sufficient glucose is provided [7].

In cancer cells, pyruvate dehydrogenase kinase (PDK) and lactate dehydrogenase (LDH) are more active than the normal cells [8]. In the presence of activated PDK, PDH is inhibited which limits the entry of pyruvate into the mitochondria. Hence, the intracellular pyruvate is converted to lactate (by LDH) instead of acetyl-CoA and thus oxidative phosphorylation is reduced. With this, the downstream mechanisms of mitochondria leading to apoptosis are down regulated, promoting the survival of cancer cells and proliferation.

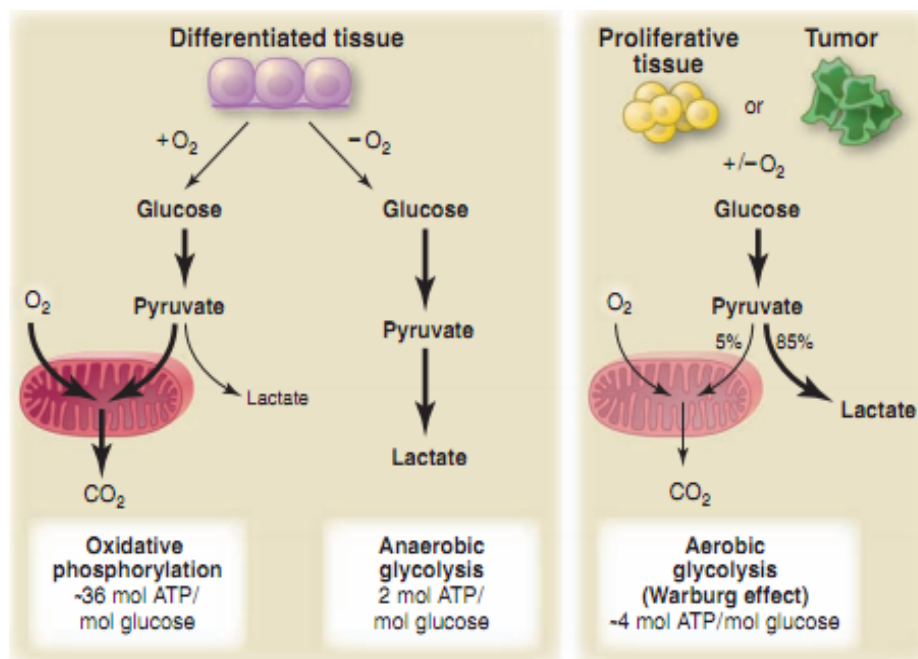


**Figure 1.3.** Schematic representation of the differences between oxidative phosphorylation, anaerobic glycolysis, and aerobic glycolysis (Warburg Effect). [Image taken from Heiden V, Science 2009]

## 1.2 Role of Warburg effect in carcinogenesis

Reprogramming energy metabolism from oxidative phosphorylation to an inefficient way — aerobic glycolysis (‘Warburg effect’) — confers a significant growth advantage to cancer cells. Carcinogenesis is a multi-step process involving many changes in the genome. The genetic changes progressively drive the transformation of normal human cells into highly malignant cells [2]. This multistep process is analogous to Darwinian evolution, wherein phenotypic properties retained or lost by the cells during genotypic alteration depend on the advantages offered to cells to survive. Gatenby and Gillies (2004) [9] have proposed that the Warburg effect confers the following advantages to cancer cells:

- The Warburg effect helps tumor cells adapt to an hypoxic environment (usually the case during early carcinogenesis) and develop into a malignant lesion.
- The Warburg effect results in increased acid production, which results in acid-induced

toxicity to normal cells in the tumor microenvironment

- The Warburg effect can reduce apoptosis
- The Warburg effect facilitates angiogenesis and metastasis

### 1.3 Dichloroacetate (DCA) as an anti-cancer drug

DCA is a chemical product of water chlorination. It is a small molecule that can penetrate most tissues after oral administration and target the mitochondria [5]. It is an inhibitor of PDKs, kinases involved in the regulation of PDH [10][11]. It can also indirectly inhibit the kinase or stimulate the phosphatase involved in the regulation of the branched-chain  $\alpha$ -keto acid dehydrogenase complex [12]. Recent work on DCA showed that it is a low price drug that is well tolerated in both adults and children and DCA is currently used in phase 3 clinical trial for patients suffering from lactate acidosis [13] [14].

In cancer cells, due to the high activity of PDK and LDH, only 5% of pyruvate enters the mitochondria while the rest undergoes aerobic glycolysis producing lactic acid. DCA has the ability to inhibit PDK activity. So, using DCA we can reverse the glycolytic phenotype in cancer cells by feeding more pyruvate into the mitochondria [11] [7]. With this the downstream pathways of mitochondria are restored leading to the production of reactive oxygen species (ROS), cyt-C, AIF and activation of caspases.

### 1.4 Metformin as an anti-cancer drug

Metformin is an anti-diabetic drug used for the treatment of patients with type II diabetes. Epidemiological studies showed that the risk of cancer in diabetic patients who had taken metformin as an anti-diabetic drug was found to be significantly lower [15][16][17]. Several *in vivo* and *in vitro* studies have highlighted the potential anti-cancer effect of metformin in various cancers in-

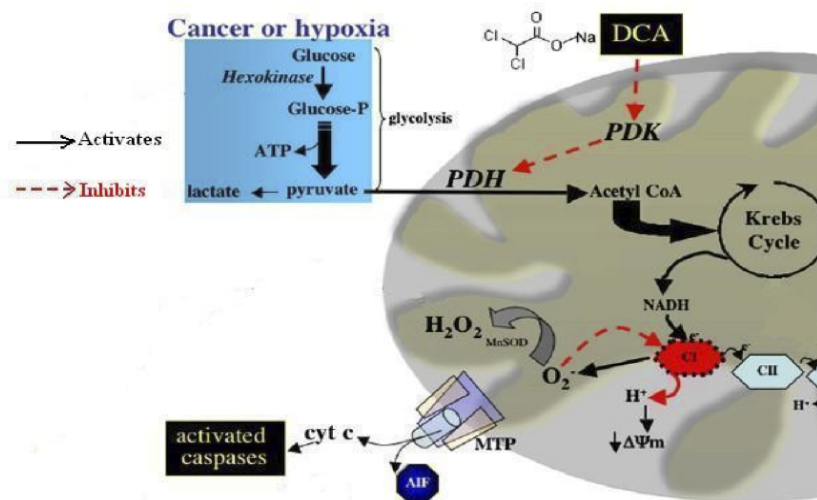


**Figure 1.4.** Remodeling of pyruvate metabolism in cancer cells by treatment with DCA. Modified from (Bonnet et al., 2007).

cluding breast cancer [18], colon cancer [19] and prostate cancer [20]. Moreover, in a case-control study of diabetic, early stage breast cancer patients treated with neoadjuvant chemotherapy, metformin users were more likely to have an absence of invasive carcinoma of the breast or axillary lymph nodes at the time of surgery indicating a higher pathological complete response than non-metformin users [21]. However, *in vitro* metformin treatment showed different effects on different subtypes of cancer cells. Most of the studies have shown that metformin inhibited cancer cell growth but did not induce apoptosis, except triple negative breast cancer cells [22] and p53 null colorectal cancer cells [19].

The molecular mechanism by which metformin exerts its anti-tumor activity is poorly understood. The primary systemic effect of metformin in diabetic patients is to lower the blood glucose levels. This is achieved by inhibition of hepatic gluconeogenesis and increased glucose uptake in skeletal muscles. Research has strongly suggested that the action of metformin in liver involves activation of adenosine 5'-monophosphate-activated kinase (AMPK) via liver kinase B1(LKB1)



[23].

### 1.4.1 The AMPK pathway

Adenosine 5'-monophosphate-activated kinase (AMPK) is a heterotrimeric serine/threonine protein kinase that acts as a cellular energy sensor. It exists in almost all eukaryotes and regulates energy balance within the cell. Mammalian AMPK comprises of a catalytic subunit ( $\alpha1$  and  $\alpha2$ ) and regulatory subunits ( $\beta1$  and  $\beta2$ ) and ( $\gamma1$ ,  $\gamma2$  and  $\gamma3$ ) [24]. It is activated in response to higher AMP/ATP ratio. There are two upstream kinases known to phosphorylate and activate AMPK, LKB1 and calmodulin-dependent kinase kinase $\beta$  (CaMKK $\beta$ ) [24] (Figure1.5).

AMPK can activate tuberous sclerosis complex 2 (TSC2) by phosphorylation which promotes Ras homolog enriched in brain (Rheb)-GTP dephosphorylation to Rheb-GDP. This inhibits mTOR complex 1 (mTORC1) [25] [26] [27] [28]. The mTOR-dependent transcriptional regulators- cyclin D1 and MYC are associated with cell proliferation and malignant progression and therefore these processes are suppressed by the activation of AMPK via mTOR dependent pathway. AMPK phosphorylation can also regulate the activity of PDK via HIF1 $\alpha$  by targeting rapamycin (mTOR) signaling pathway [8] (Figure1.5).

Although the molecular mechanisms of metformin has been studied in liver, muscle and fat tissues, little has been done to understand the mechanism behind the anti-cancer activity of metformin. The recent studies have shown metformin's activity on cancer cells to be dependent on the LKB1-AMPK pathway in some cell lines [19] [29] but independent in others. Ben Sahara *et al.* 2008 [30] showed that metformin activated the AMPK pathway in human prostate cancer cells but mediated its effect independently of the AMPK pathway. Other studies found that the activation of AMPK is a response to inhibition of complex I of mitochondrial electron transport chain by metformin [31] [32].

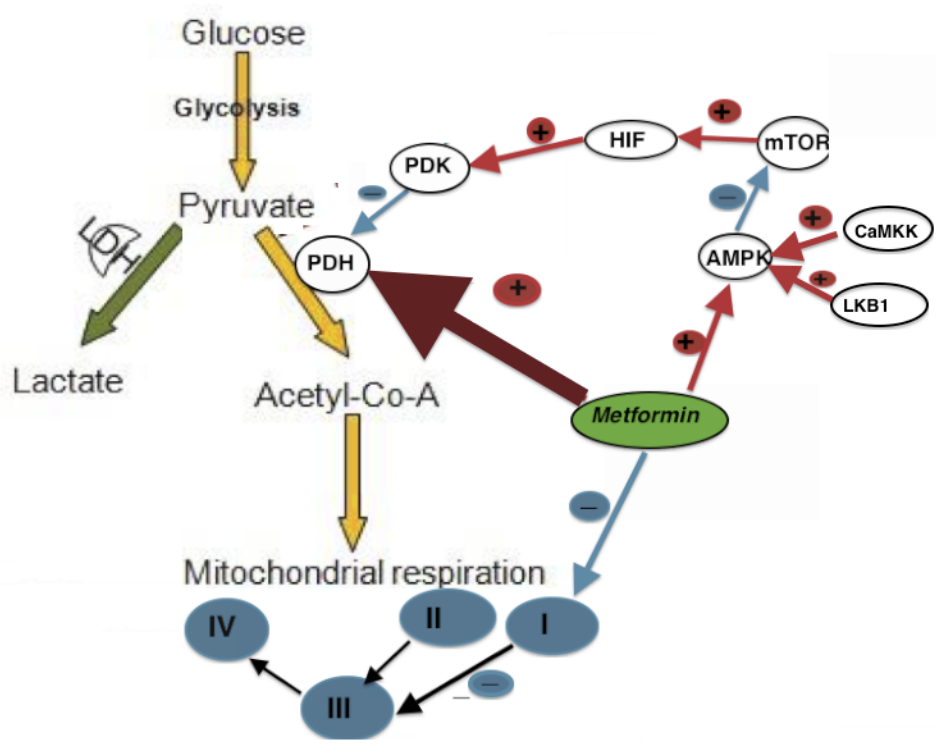
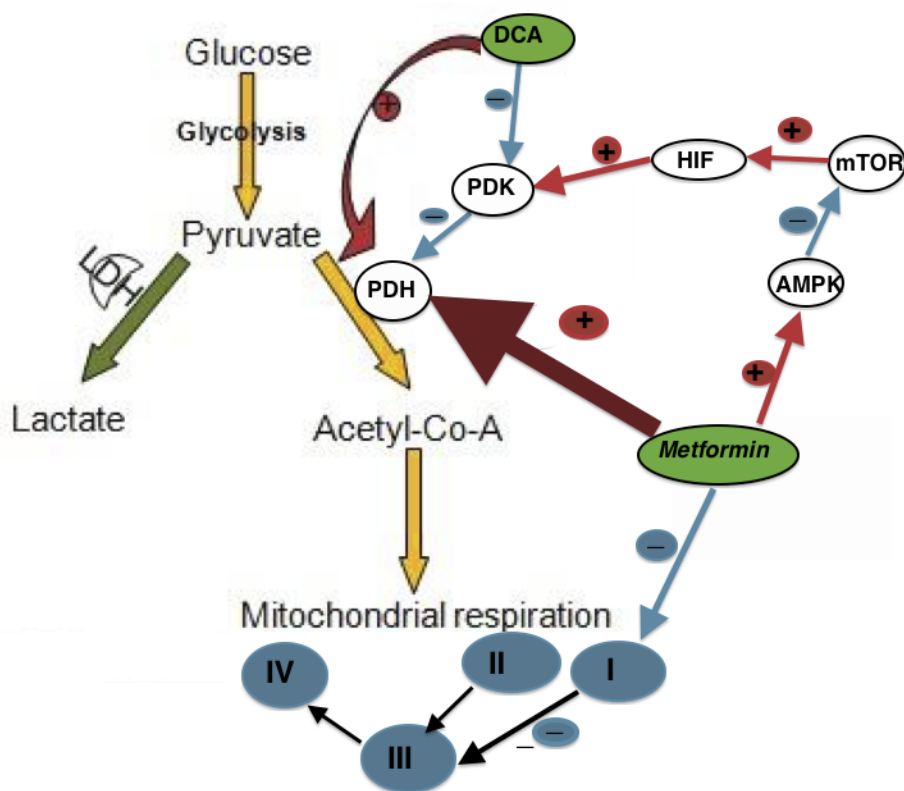


Figure 1.5. Targets of metformin and AMPK pathway.

## 1.5 Combination treatment of breast cancer with metformin and DCA

Recent studies have focused on the role of metformin and DCA individually in inhibiting proliferation of tumors of diverse origin. DCA has been suggested as a novel and relatively non-toxic anticancer agent [5] [11]. It can directly inhibit the activity of PDKs and direct more pyruvate into the mitochondria. On the other hand, metformin inhibits complex I of the respiratory chain. While both DCA and metformin inhibit the activity of PDKs, DCA targets PDKs directly but metformin targets HIF1 $\alpha$  through AMPK-mTOR pathway, which then targets PDKs. Therefore, the combination of the two drugs will reverse the aerobic glycolysis to oxidative phosphorylation



**Figure 1.6.** Remodeling of cancer metabolism with metformin and DCA.

in cancer cells. Moreover, the combination of two drugs can have synergistic activity and be particularly toxic to cancer cells as we are redirecting metabolism into mitochondria with one drug while inhibiting the ETC with a second drug. This leads to reduced ATP production, which disrupts energy homeostasis in cells and increases metabolic stress.

The anti-tumor effect of metformin is seen, however at concentrations ( $>1\text{-}5\text{mM}$ ), at least 100 fold above the plasma concentration range ( $6\mu\text{M}$ -  $30\mu\text{M}$ ) achieved in type II diabetic patients taking metformin [22]. The dose of DCA used in the study is non-toxic to normal cells [11]. When cancer cells are treated with metformin and DCA in combination, DCA might boost the effectiveness of metformin even at a lower dosage, such as at the level used for type II diabetes. Also, the two drugs are non-toxic, cheap and already used in clinics for other illness and can

easily go on to clinical trial for prevention therapy.

### **1.5.1 Hypothesis and specific aims**

bf Metformin and DCA in combination can reverse the glycolytic phenotype in tumor cells and increase metabolic stress for cells and hence slower the growth rate (Figure1.6).

#### **1.5.1.1 Specific Aims**

- To examine the efficacy of metformin and DCA on V14 breast cancer cell line
  - Measure the total cell number after drug treatment
    - \* Neutral Red Assay and IncuCyte
  - Check the expression/activation of drug targets
    - \* Western blotting for AMPK, pAMPK for metformin
    - \* Measure the level of lactate to assess action of DCA on PDKs
  - Assess mitochondrial metabolic activity
    - \* Measure the amount of ATP produced

# Chapter 2

## Materials and Methods

### 2.1 Cell lines and culture conditions

The V14 cell line is a *Trp53*<sup>-/-</sup> cell line derived from spontaneous mammary adenocarcinoma in a BALB/*c Trp53*<sup>+/-</sup> mouse by Dr. Anneke Blackburn [33]. It was grown in DMEM/F-12 (Invitrogen CO CA, USA) medium supplemented with 25mM Hepes (MP Biomedicals, USA), 2% adult bovine serum (ABS), 0.1% PSN (3% penicillin, 5% streptomycin and 5% neomycin), 5ng/ml epidermal growth factor (EGF), 10 $\mu$ g/ml insulin, 15 $\mu$ g/ml gentamicin (Sigma, Mo, USA). PSN was obtained from Media/Wash-up, John Curtin School of Medical Research, The Australian National University, Australia. The cells were cultured at 37°C in 5% CO<sub>2</sub> in T25, T75 or T175 filter cap tissue culture flasks (Nunc, Denmark).

### 2.2 Drug treatment

DCA(Sigma-Aldrich, USA) stock solution (100mM) was prepared in PBS and neutralized to pH 7 with NaOH, filter sterilized and stored at 4°C. Metformin(Sigma-Aldrich, USA) stock solution (25mM) was also prepared in PBS, filter sterilized and stored at 4°C. 5-aminoimidazole-

4-carboxamide 1- $\beta$ -D-ribofuranoside (AICAR) stock solution (25mM) was prepared in PBS, filter sterilized and stored at  $-20^{\circ}\text{C}$ . AICAR was a gift from Professor Michael Djordjevic's lab, Research School of Biology, The Australian National University. Different concentrations of drugs were prepared by diluting the stock in fresh media on the day of treatment.

### **2.3 Cell proliferation assay**

Cell proliferation was examined using IncuCyte-live cell imaging system (ESSEN INSTRUMENTS, Ann Arbor, MI, USA). It provides real time information on the changes in cell number that occur over the course of time. V14 cells were plated in 96-well plates at a plating density of 10,000 cells per well. The next day, cells were treated with various concentrations of DCA and metformin alone and in combination in 4 replicates. Measurements of cell monolayer confluence were obtained by phase-contrast images every 2 hours over 72 hours using IncuCyte. Outliers were removed manually and data was further processed using Microsoft Excel and Stata.

### **2.4 Neutral red cell viability assay**

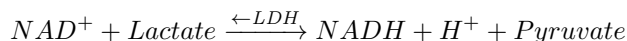
Neutral red assay provides a quantitative estimation for the number of live cells present in a well. Neutral red dye is taken up by viable cells which binds to the lysosomes. When cells are lysed, the absorbance of neutral red at 540nm is proportional to the total number of viable cells [34]. Neutral red assay was done after 72 hours of drug treatment, after IncuCyte data was collected. It was done to validate IncuCyte results. Neutral red(Sigma, USA) ( $30\mu\text{g}/\text{ml}$ ) was made in fresh media and was added to each well. After 3 hours incubation at  $37^{\circ}\text{C}$ , cells were washed twice with PBS. Then, lysis buffer (acetic acid 75% and methanol 25%) was added into each well. The absorbance at 540nm was determined using SpectraMAX 190 spectrophotometer (Molecular Devices, CA, USA).

## 2.5 Analysis of drug interaction

The effect of the combination of metformin and DCA was evaluated using the method initially described by Kern *et al.* [35] and later modified by Romanelli *et al.* [36]. Briefly, R Index (RI) value was calculated as a ratio of the expected cell survival  $S_{exp}$  to the observed cell survival  $S_{obs}$  ( $RI = S_{exp} / S_{obs}$ ).  $S_{exp}$  is defined as the product of the survival observed with drug A and drug B alone.  $S_{obs}$  is defined as the cell survival observed for the combination of drug A and B.  $RI < 1$  indicates antagonistic effect,  $RI = 1$  indicates additive effect and  $RI > 1$  indicates synergistic effect.

## 2.6 Lactate assay

Lactate level in the media was assessed spectrophotometrically in 96 well plates using Spectra-MAX 190 spectrophotometer (Molecular Devices, CA, USA) at 340nm.



The fundamental principal of lactate assay lies in the above equation. The lactate is converted to pyruvate and  $NAD^+$  into NADH. At a high pH and a higher concentration of  $NAD^+$ , it is possible to push the above reaction towards the right. Lactate stoichiometrically reduces  $NAD^+$  to NADH, and the amount of lactate in the sample can be measured using change in optical density at 340nm against a standard curve for lactate prepared from Sodium L-Lactate (Sigma-Aldrich, USA) [37].

Media samples (75 $\mu$ l) were collected at different time points and frozen until assay was performed. Perchloric acid (PCA) (225 $\mu$ l of 4% solution) was added to the standards and samples on ice to deproteinize the media samples. Methyl orange (5 $\mu$ l of 0,05% w/v) was added as a pH indicator. The PCA extract was neutralized by adding 80 $\mu$ l of 1M potassium carbonate ( $K_2CO_3$ ). This was the volume predetermined to change the methyl orange from pink to yellow,

indicating neutral pH. Water (15 $\mu$ l) was added giving a final volume of 400 $\mu$ l. Neutralized extracts of samples and standards (40 $\mu$ l) were pipetted into a 96-well plate on ice. Then, 100 $\mu$ l of glycine hydrazine buffer (2g hydrazine sulfate, 7.5g glycine, 0.2g EDTA in 49ml of H<sub>2</sub>O and 51ml of 2M NaOH), 40 $\mu$ l of 5mM NAD<sup>+</sup>, 30 $\mu$ l of H<sub>2</sub>O and 10 $\mu$ l of rabbit L-lactate dehydrogenase (LDH) (Sigma Co, MO, USA) was added to each well. The change in absorbance at 340nm was recorded before and after the addition of LDH using SpectraMAX 190 spectrophotometer. The lactate concentration was obtained by calculating the change in absorbance over 40mins and comparing the values to a standard curve of lactate.

## 2.7 Western blotting

Cells were harvested and total proteins were extracted using M-PER Mammalian Protein Extraction Reagent buffer (Thermo-Scientific, IL, USA) containing protease inhibitor (Protease Inhibitor Cocktail tablets, Roche, Mannheim, Germany) and phosphatase inhibitor (Phosphatase Inhibitor Cocktail Set V, EMD Biosciences, CA, USA). Protein extracts (60 $\mu$ g) was loaded onto 10% SDS-poly acrylamide gels. The resolved proteins were transferred electrophoretically to polyvinylidene fluoride (PVDF) membrane. Membranes were then blocked for an hour with 5% bovine serum albumin (BSA) in tris-buffered saline (TBS) buffer containing 0.05% Tween-20 (TBST). Immunoblotting was performed overnight at 4°C with antibodies against AMPK phosphorylated on Thr172 (1:500) and total AMPK $\alpha$  (1:1000) (Cell Signaling Technology, Danvers, MA, USA; Cat no: 2535 and 2603). The membranes were then washed in TBST and incubated with secondary antibodies (HRP conjugated goat anti-rabbit polyclonal Ab, DAKO # P0448) for an hour. Membranes were again washed briefly with TBST and RapidStep ECL Reagent (Calbiochem, USA) was sprayed on the membrane and films were developed using Kodak X-OMAT 1000 processor (Kodak, USA).  $\beta$ -actin (Abcam #ab8227) was used as a control for loading.



## 2.8 Cell metabolism

Internal ATP levels in V14 cells were assessed at different time points using CellTiter-Glo assay (Promega Corp., Madison, WI). According to the kit protocol, cells were seeded in a white opaque 96 well plate at 15,000 cells/well in 50 $\mu$ l of media, incubated overnight and then treated with various concentrations of DCA and metformin alone and in combination for 4 hours and 24 hours at 37°C. CellTiter-Glo reagent (50 $\mu$ l) was added and incubated at room temperature for 10 min. Glomax micro-plate luminometer (Promega Co., WI, USA) was used to detect the luminescence.

## 2.9 Apoptosis assay

Caspase 3/7 activities in V14 cells were assessed at different time points using Caspase 3/7 assay (Promega Corp., Madison, WI). According to the manufacturer's instructions, cells were seeded in a white opaque 96 well plate at 15,000 cells/well in 50 $\mu$ l of media. Cells were allowed to adhere overnight before drug treatment was started. Caspase 3/7 activity was measured after 4 hours and 24 hours of drug treatment. Staurosporine (Sigma-Aldrich, USA) (1 $\mu$ l) which can induce apoptosis was added as a positive control. Caspase 3/7 reagent (50 $\mu$ l/per well) was added and incubated at room temperature for 30 min. Glomax micro-plate luminometer (Promega Co., WI, USA) was used to detect the luminescence.

## 2.10 Statistical analysis

Students t-test was used to assess differences between drug treated and control groups. A P value of less than 0.05 was considered to be statistically significant. Data are represented as mean + standard error. Robustness of the cell viability data was checked using classical measurement error model.

## Results

### 3.1 Metformin and DCA treatment in combination is more effective at reducing cell proliferation *in vitro*

To investigate if metformin and DCA can independently affect V14 cell proliferation, we used IncuCyte system to monitor real time cell growth over 72 hours and neutral red assay to assess cell viability (Figure 3.1 – 3.4). Interestingly, the lower doses of metformin (0.02mM and 0.1mM) showed a protective effect while continuous exposure to higher doses had significant reduction in cell number (Figure 3.1 and 3.2). Similarly, continuous exposure to DCA at 5mM inhibited cell proliferation, however, treatment with lower concentrations (0.2, 0.1, 1mM) did not result in the same inhibition (Figure 3.3, 3.4).

To determine the synergistic effect of metformin combined with DCA in reducing cell proliferation, first  $IC_{50}$  for each drug alone for 72 hours treatment was determined using MATLAB.  $IC_{50}$  is defined as the drug concentration leading to a 50% inhibition of cell growth. The  $IC_{50}$  value for metformin alone was 3mM and that for DCA alone was 5.2mM (Figure 3.5). The synergy between the two drugs was then evaluated using the R index method. For the combination

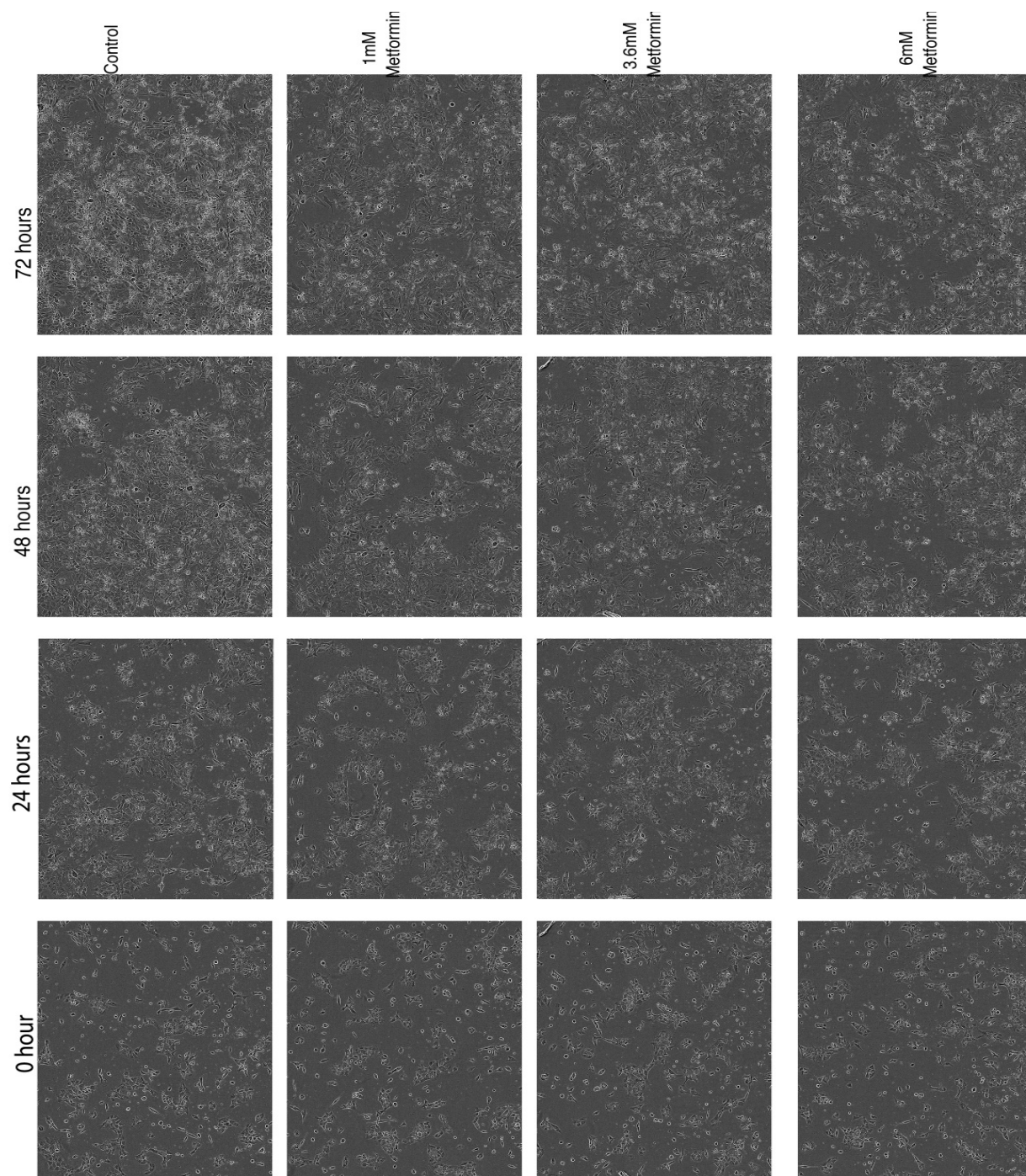


**Figure 3.1.** Effect of metformin on V14 cells. Images taken by IncuCyte at different time points, 24h, 48h and 72h show that there is reduction in cell number after metformin treatment.

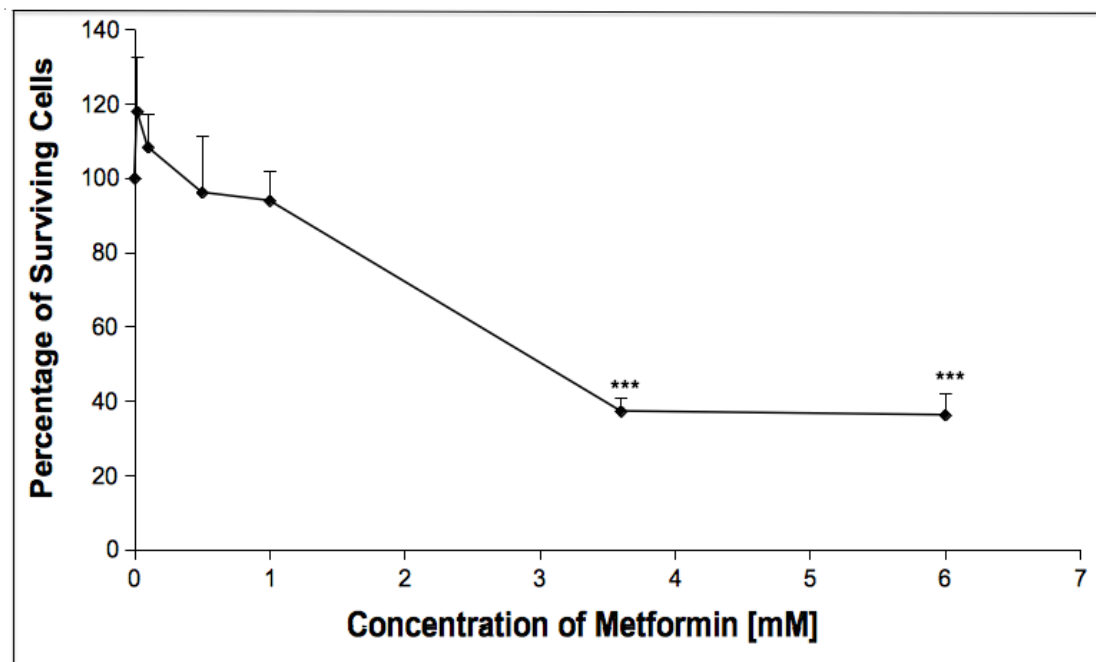


**Figure 3.2.** Effect of metformin on V14 cells. The percentages of surviving cells relative to control, defined as 100% survival, were determined by neutral red assay. Data shows the mean of four independent experiments + SEM. \*\*\* $P < 0.005$  versus control.

treatment, we only considered the lower doses of metformin, as one of our aims was to enhance the anti-tumor activity of metformin at a lower concentration. With 1mM and 5mM DCA, a synergistic effect was observed with 0.5mM and 1mM of metformin (Figure 3.6). There was at least 4 fold decrease in viable cells when 5mM DCA was combined with 0.5mM and 1mM metformin, compared with just metformin treatment alone (data not presented). These results suggest that DCA enhanced the anti proliferative effect of metformin. The three-dimensional log-log surface plot (Figure 3.7) visually depicts the interaction between the two drugs at various concentrations.

### 3.2 Metformin and DCA do not induce apoptosis

At the heart of apoptotic pathway lies a family of cysteine proteases, the ‘caspases’. To examine if metformin and DCA promoted apoptosis, we quantified apoptosis by measuring proapoptotic

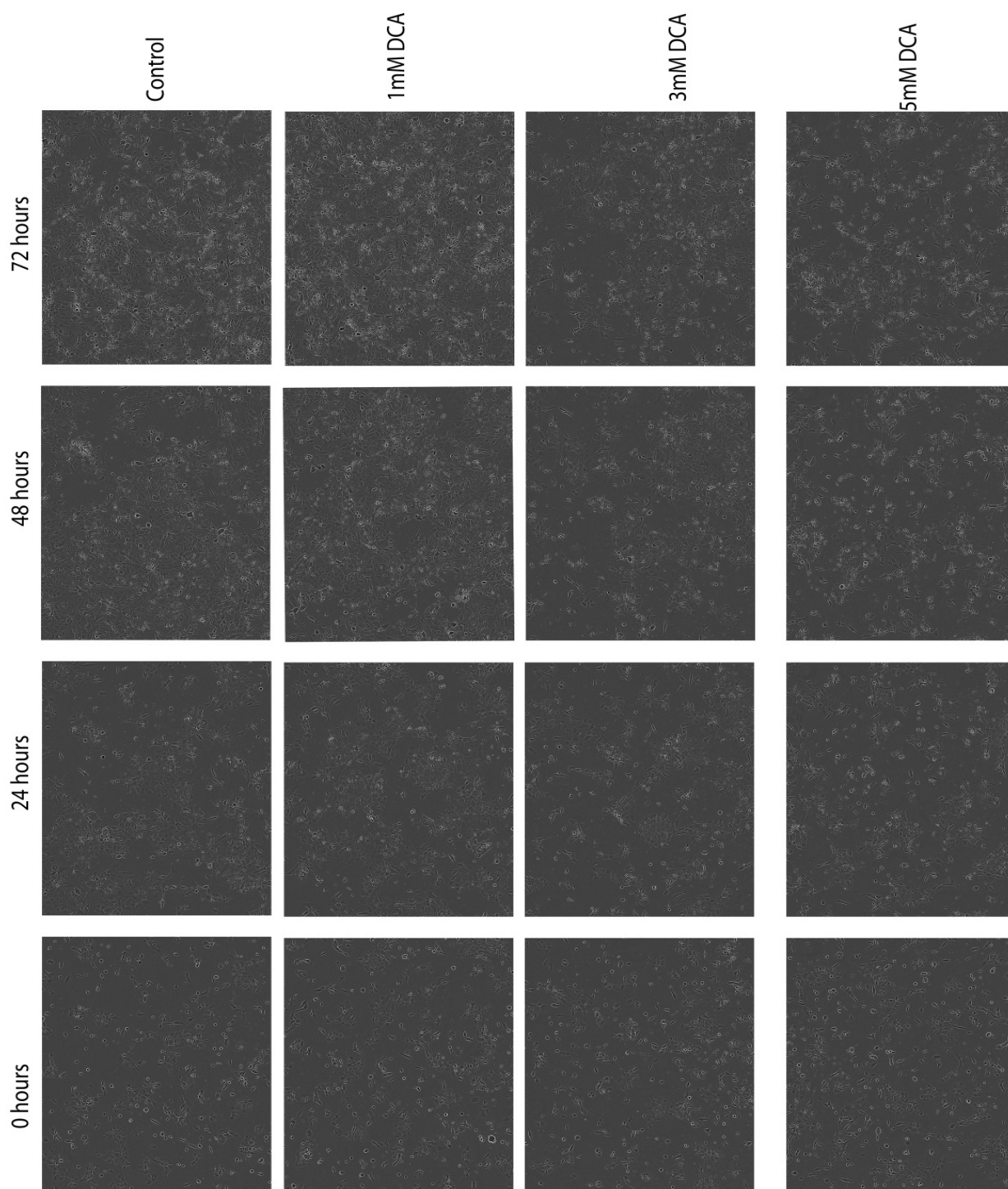


**Figure 3.3.** Effect of DCA on V14 cells. Images taken by IncuCyte at different time points, 24h, 48h and 72h show that there is reduction in cell number after DCA treatment.

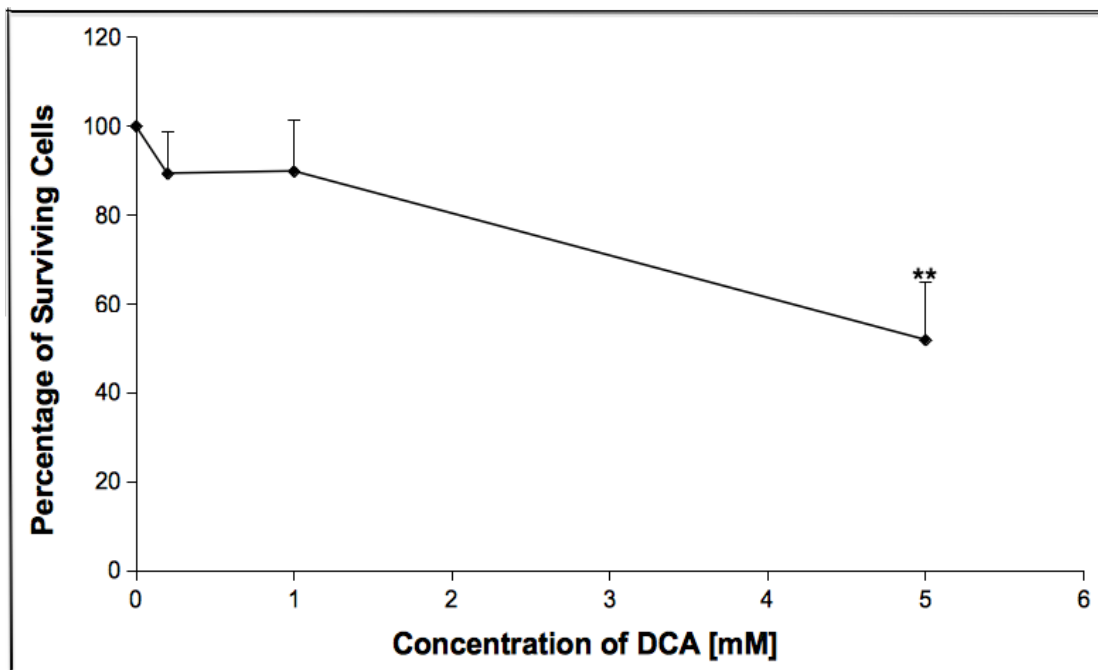


**Figure 3.4.** Effect of DCA on V14 cells. The percentages of surviving cells relative to control, defined as 100% survival, were determined by neutral red assay. Data shows the mean of four independent experiments + SEM. \*\*P < 0.01 versus control.

protein caspase 3 and 7 activation. As shown in Figure 3.8, treatment of V14 cells with DCA and metformin alone or in combination resulted in no significant increase in caspase 3 and 7 activity. However, there was 4 fold increase in caspase activity after the cells were treated with  $1\mu\text{M}$  of staurosporine, a cytotoxic drug.

### 3.3 Metformin and DCA both increase AMPK activity

We did immunoblotting of activated AMPK (p-AMPK) and total AMPK levels to examine if metformin was acting on its molecular target. As expected metformin increased the level of activated AMPK (p-AMPK) without changing total AMPK levels in a dose dependent and time dependent manner. Unexpectedly, DCA also activated AMPK in a dose dependent and time dependent manner (Figure 3.9). Moreover, 5mM DCA enhanced the activation of AMPK by 6mM metformin, however the same effect was not observed with lower dose (1mM) of metformin

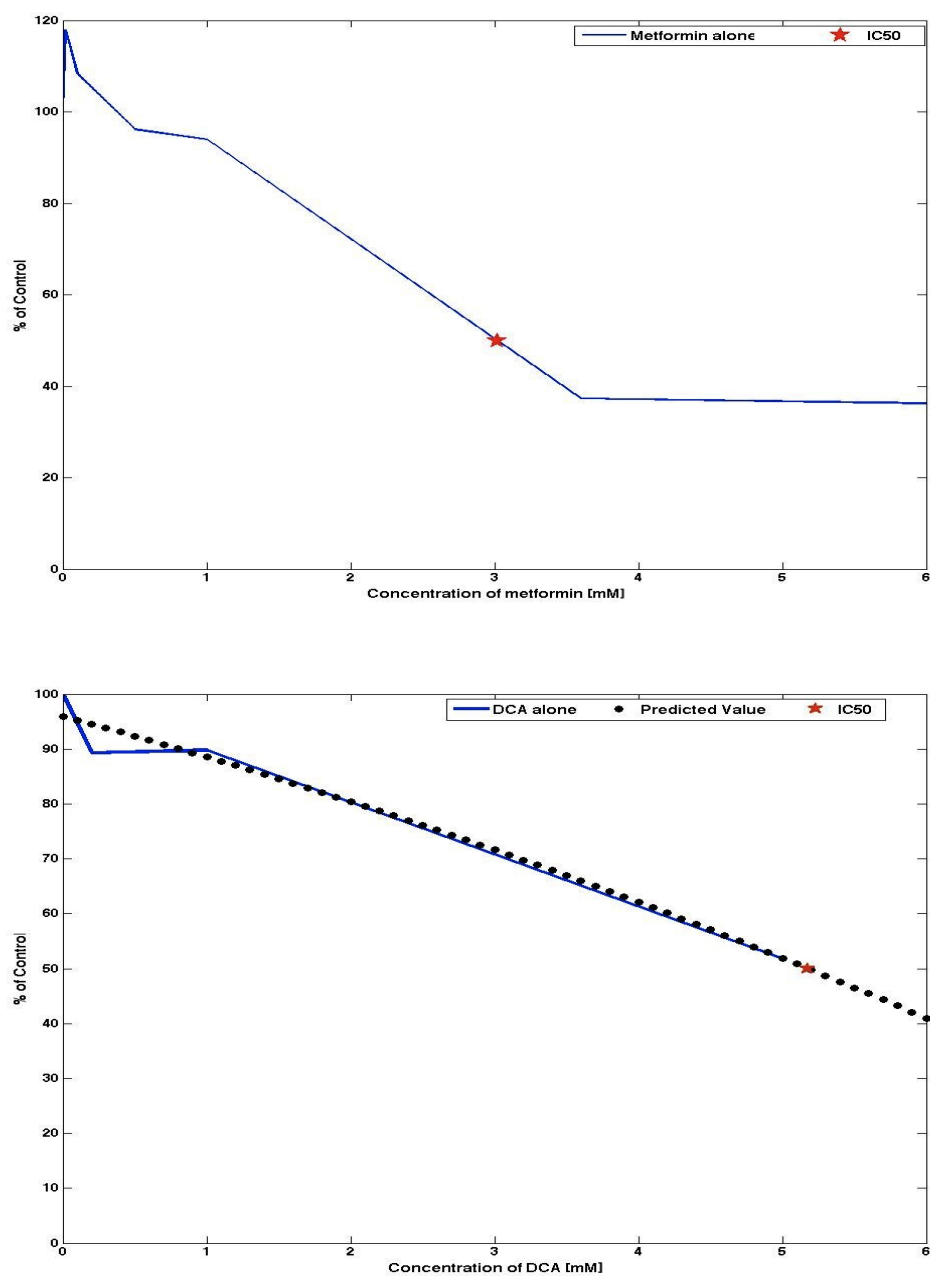


**Figure 3.5.** Interpolation of  $IC_{50}$  of DCA and metformin on V14 cell lines after 72 hours exposure.  $IC_{50}$  is defined as the drug concentration leading to a 50% inhibition of cell growth. Interpolation was done using MATLAB inbuilt function. Data represents the average of four independent experiments.

(Figure 3.9). DCA increases the ATP/AMP ratio in the cells which is inversely related to AMPK activation. Activation of AMPK with DCA highlights other pathways in which DCA might be

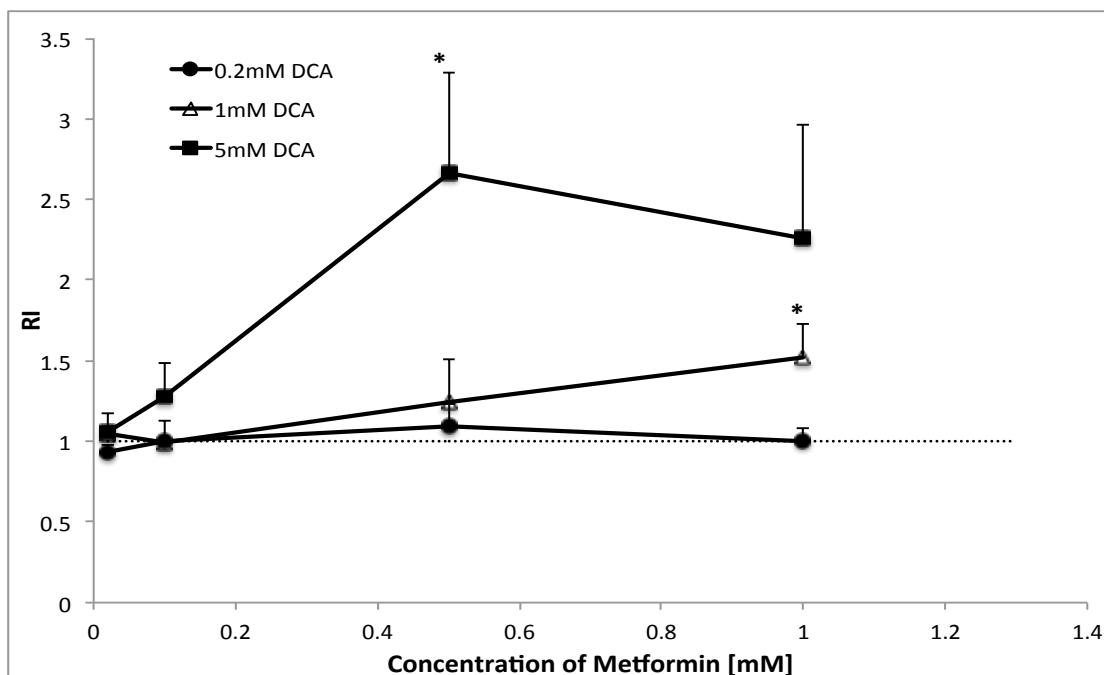


**Figure 3.6.** Evaluation of interaction between DCA and metformin after 72 hours exposure. RI values were calculated from neutral red cell viability assay. Synergism is defined as  $RI > 1$ . Values are expressed as mean + SEM,  $n=4$ . Significant difference was assessed using t-test, with null hypothesis  $RI=1$ . \* $P < 0.05$ .

acting in the cells.

A commonly used downstream target of AMPK is acetyl-coenzyme A (CoA) carboxylase (ACC)-2. AMPK is known to phosphorylate and inactivate ACC-2. ACC-2 is an isoform of ACC that produces malonyl-CoA in the mitochondrial-inner membrane space. Malonyl-CoA is an inhibitor of fatty acid uptake. Phosphorylated ACC (p-ACC-2) inhibits the production of malonyl-CoA, increasing fatty acid uptake (fatty acid oxidation). *In vivo* study of DCA done by our lab (results not published) (Figure 3.10) showed that p53 heterozygous mice treated with DCA had lower weight than the control, indicating that DCA might have increased the fatty acid oxidation via AMPK, ACC pathway. This provides further evidence that DCA not only targets PDK, but also acts on a different pathway that activates AMPK.



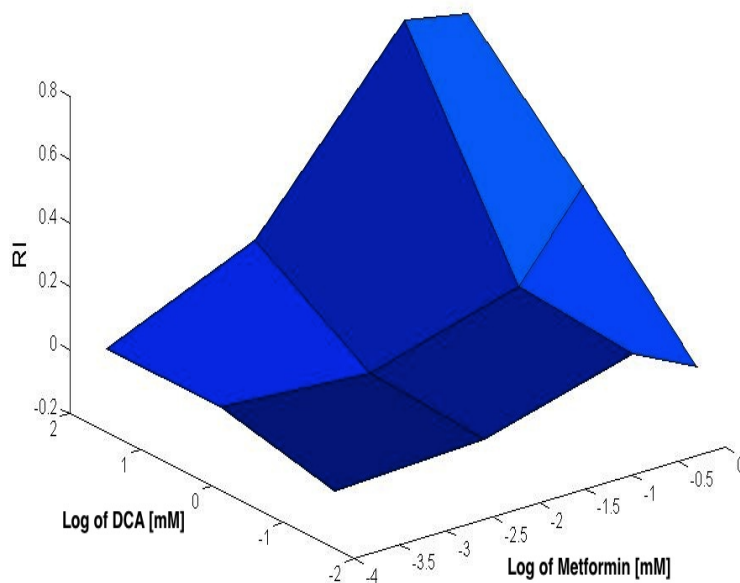


**Figure 3.7.** Three dimensional log-log surface plot representing the interaction between DCA and metformin after 72hours exposure.

### 3.4 DCA reverses the Warburg effect while metformin inhibits complex I of ETC, disrupting the energy homeostasis

DCA treatment inhibits PDK activity and increases mitochondrial metabolism [11] while metformin treatment blocks complex I of ETC and impairs mitochondrial respiration [19]. Inhibition of PDK by DCA leads to increasing conversion of pyruvate into acetyl-coA and decreases lactate production but inhibition of complex I stimulates glycolysis to maintain cellular bioenergetics [19]. To examine the activity of DCA and metformin on mitochondrial respiration, we measured extracellular lactate level and ATP production. As expected, treatment of V14 cells with DCA reduced the lactate production in a dose-dependent manner. After 4 hours of DCA treatment, extracellular lactate concentration was decreased by 14.6% with 1mM DCA, however the effect diminished over time, with only 6% reduction after 24 hours of treatment. Higher dose of DCA,

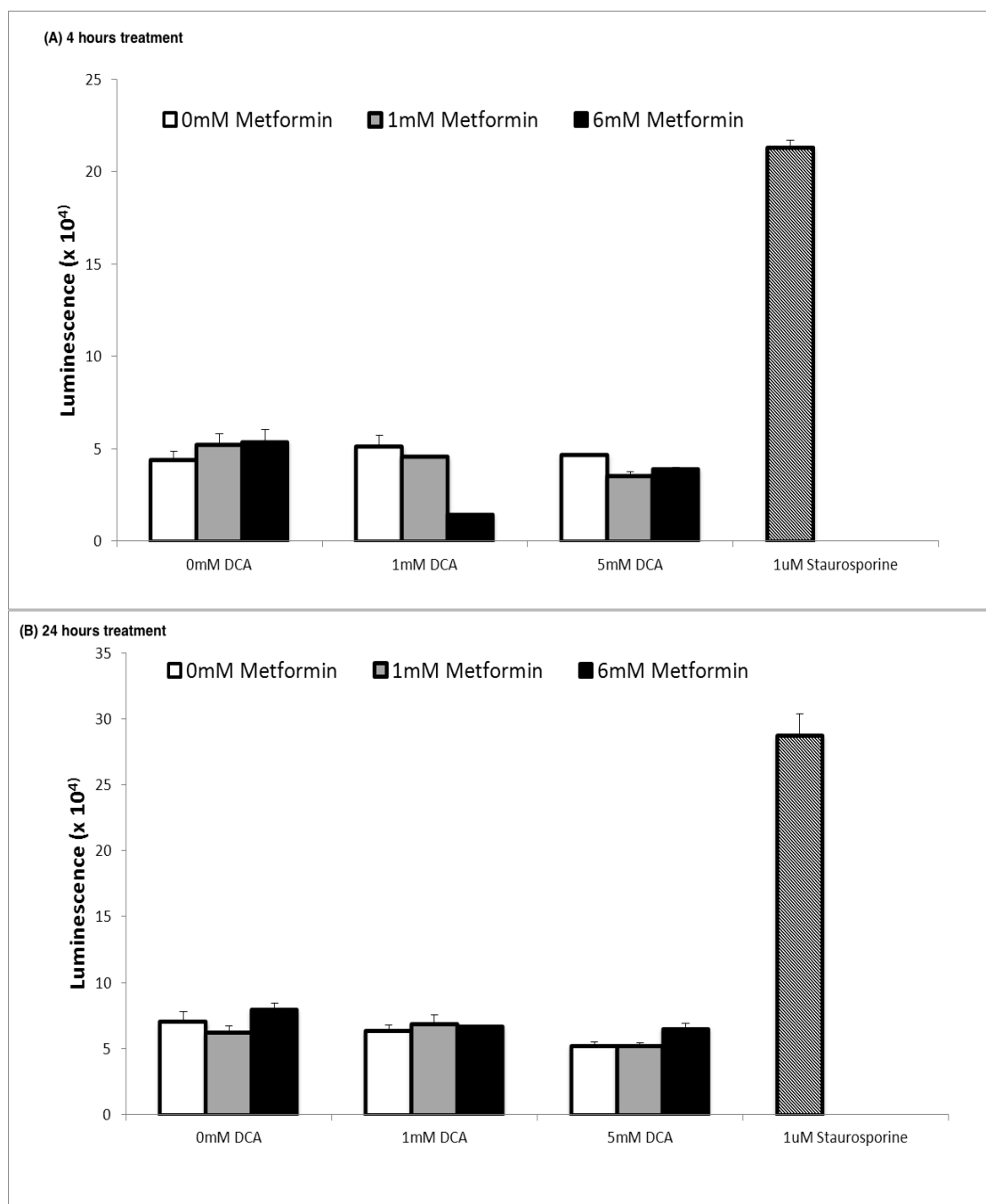


**Figure 3.8.** Metformin and DCA treatment, individually or in combination, did not increase caspase 3 and 7 activity significantly. (A) Caspase 3 and 7 activity after 4 hours of treatment. (B) Caspase 3 and 7 activity after 24 hours of treatment. 1 $\mu$ M Staurosporine is used as a positive control. Values are expressed as mean + SEM, n=3.

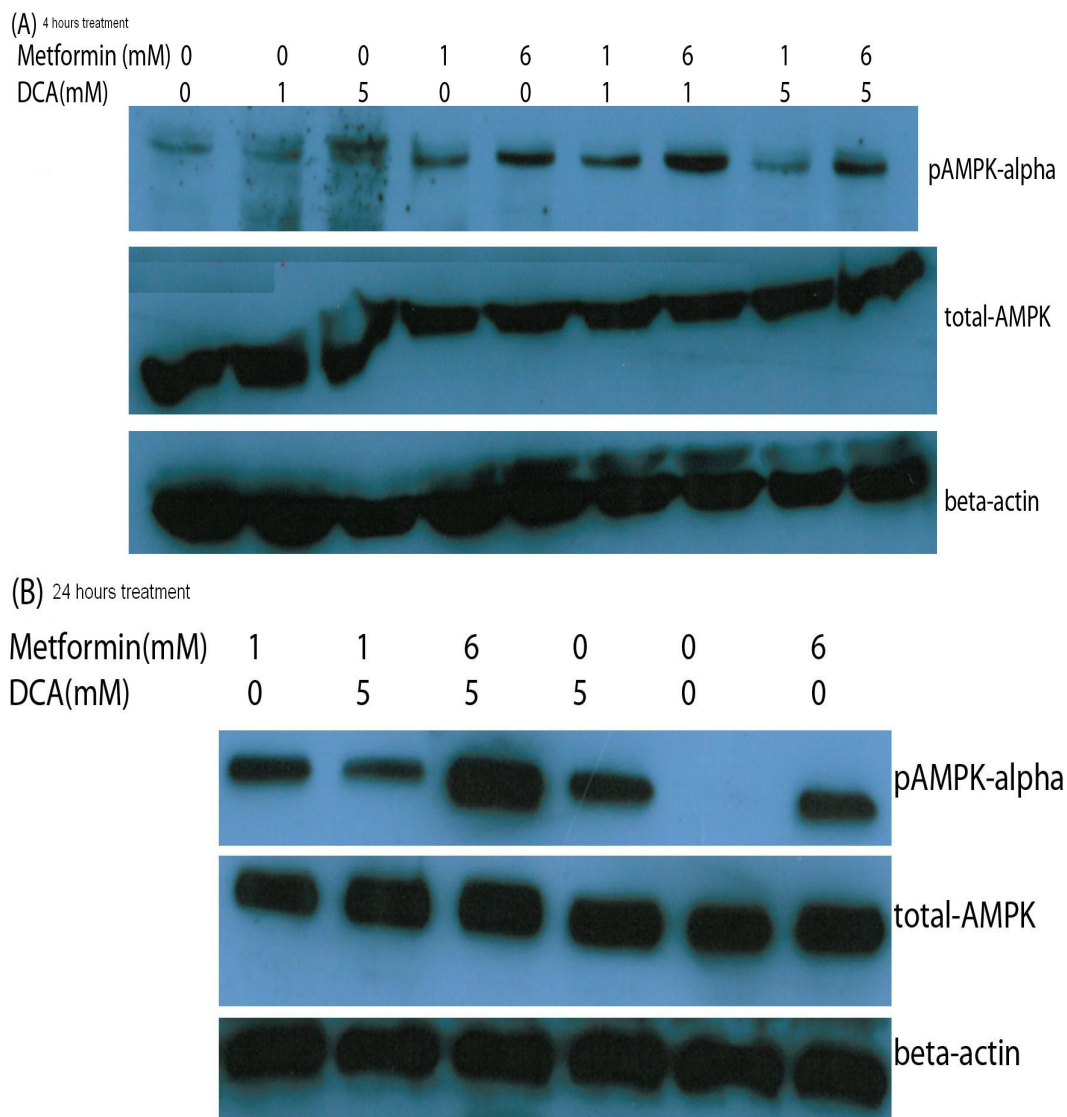


**Figure 3.9.** Metformin and DCA activates AMPK in a dose-dependent manner. V14 cells were treated with DCA and metformin alone and in combination for 4 hours (A) and 24 hours (B). Phosphorylation of AMPK at (Thr<sup>172</sup>) was measured by western blot.  $\beta$ -Actin is shown as loading control.

5mM reduced the lactate production by 33.8% after 4 hours of treatment and this effect persisted at 24 hours (Figure 3.11).

Metformin treatment showed a small (28%) but statistically significant increase in lactate production after 24 hours. To address whether the increased lactate production was due to inhibition of complex I and not dependent on AMPK activation, we treated V14 cells with another AMPK activator AICAR, which directly activates AMPK and is not known to effect mitochond-

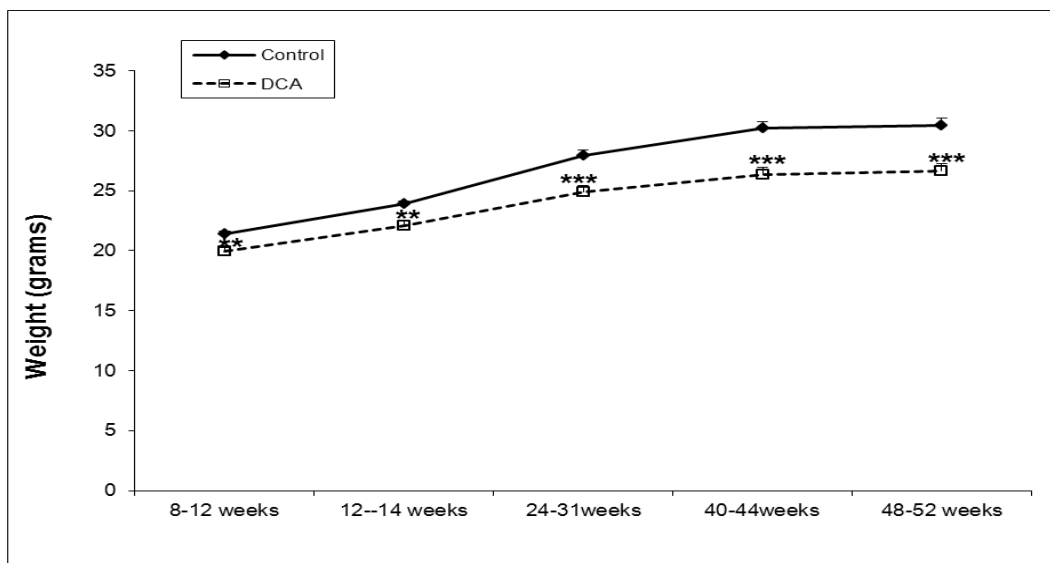


**Figure 3.10.** DCA treatment reduced the weight of p53 heterozygous mice. p53 heterozygous mice were put on DCA treatment when they were 4 weeks old until the spontaneous tumor that they developed reached about 1.2 cm in radius. The control group were put on normal water and sacrificed when their spontaneous tumor grew about 1.2 cm in radius. \*\* $P < 0.01$ , \*\*\* $P < 0.005$  versus control.

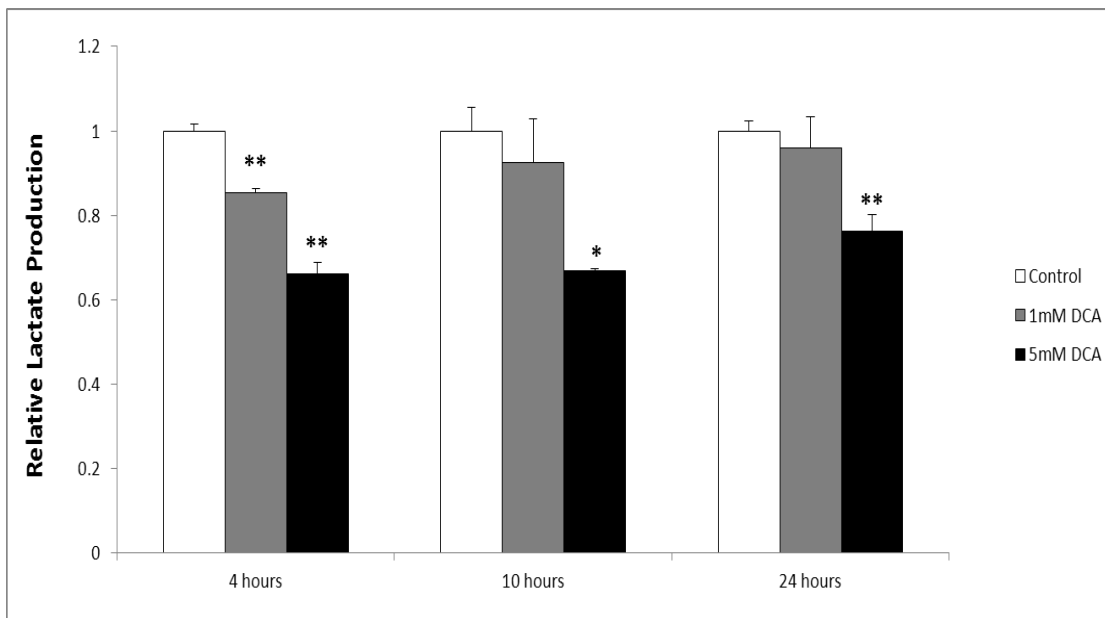


**Figure 3.11.** Effect of drug treatment on extracellular lactate levels. Relative lactate concentration after 4 hours, 10 hours and 24 hours of DCA treatment. Values are expressed as mean + SEM,  $n=3$ . \* $P < 0.05$ , \*\* $P < 0.01$  versus control.

drial metabolism. AICAR treated cells did not show any significant change in lactate production (Figure 3.12), suggesting metformin induced lactate production is due to the inhibition of Com-

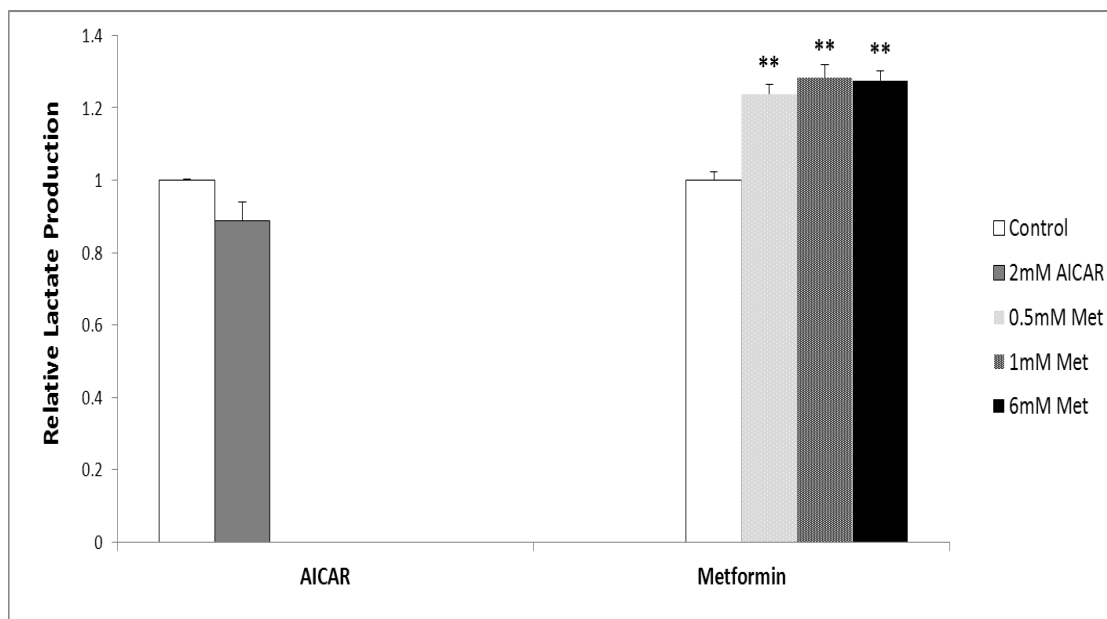


**Figure 3.12.** Effect of drug treatment on extracellular lactate levels. (A) Relative lactate production after 24 hours of treatment with AICAR and metformin. Values are expressed as mean + SEM, n=3. \*\*P<0.01 versus control.

plex I and not related to activation of AMPK.

To determine if DCA and metformin mediated change in mitochondrial respiration may disrupt energy homeostasis, we examined the level of ATP production after drug treatments. Treatment of V14 cells with DCA for 4 hours resulted in an increase in ATP levels(Figure 3.13a). With 5mM of DCA, there was 17% increase in the ATP levels, which is consistent with reversal of the glycolytic phenotype. Interestingly, DCA mediated increase in ATP levels didn't last after 24hrs treatment, indicating the adaptation of cells to the presence of DCA. On the other hand, metformin decreased the ATP level in a dose and time dependent manner consistent with inhibition of complex I of the ETC. Combined treatments decreased overall ATP levels in V14 cells after 4 hours of treatment and this result was persistent after 24 hours treatment(Figure 3.13). The level of highest reduction was seen with 6mM metformin combined with 5mM DCA.

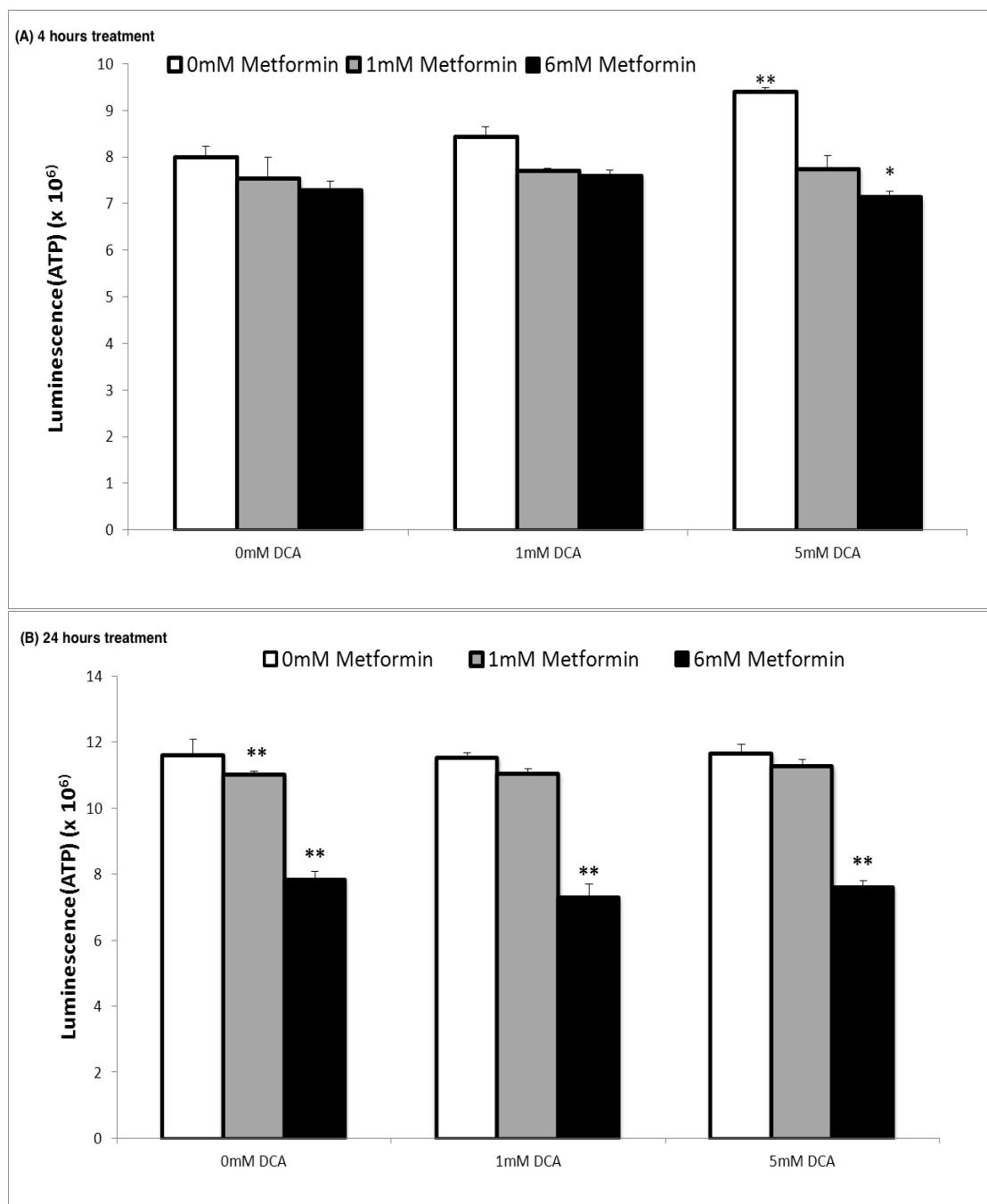


**Figure 3.13.** Effect of drug treatment on ATP levels. (A) ATP levels after 4 hours of treatment. (B) ATP levels after 24 hours of treatment. Values are expressed as mean + SEM, n=3. \*P<0.05, \*\*P<0.01 versus control.

# Chapter 4

## Discussion

### 4.1 Summary

Recent epidemiological study of type II diabetic patients has shown that metformin treatment reduces the cancer incidence and mortality in these patients [15][16][17]. On the other hand, DCA due to its ability to inhibit PDK activity and reverse the glycolytic phenotype, has attracted much attention in the scientific community. The purpose of this study was to remodel the metabolism of the V14 p53<sup>-/-</sup> breast cancer cell line using DCA and metformin and characterize the effects of the drug treatment on their targets or on cell survival and proliferation. We report that treatment with either metformin or DCA reduces the growth of V14 breast cancer cells *in vitro*. Measurement of caspases 3 and 7 activity clearly demonstrated that this was due to inhibition of proliferation, with no signs of apoptosis. This contrasts with the results published by Buzzai *et al* [19] where they reported that metformin selectively killed p53<sup>-/-</sup> colon cancer cells *in vivo* and *in vitro*. It also contrasts with studies published on DCA treatment of endometrial, prostate and lung cancer cells where they reported increased apoptosis with no effect on cell cycle distribution [38] or increased apoptosis accompanied by decreased proliferation [5]. The mechanism by which metformin and DCA affect cell cycle arrest and tumor growth are not fully understood. This

will be the subject of further investigation.

Moreover, there was at least 4 fold decrease in viable cells when 5mM DCA was combined with 0.5mM and 1mM metformin, compared with metformin treatment alone. Therefore, DCA (5mM) enhanced the anti-tumor activity of metformin at 0.5mM, a concentration higher than the plasma concentration range found in type II diabetic patients, but much lower than the  $IC_{50}$  of metformin alone reported in the literature and from our results. DCA treatment increased the ATP levels in V14 cells after 4 hours treatment, but this result was not persistent over 24hours. Similarly, the lactate level was reduced with 4 hours DCA treatment but this effect diminished over time. While DCA is affecting its targeted molecule (PDK) and reversing the 'Warburg Effect' as seen from ATP and lactate results, the effect seems to be an immediate effect which vanishes over time. However, with metformin treatment we found that the effect is dose and time dependent. This suggests that DCA's effect is an immediate effect and that it gets metabolized quickly however, metformin remains in the media and has a long term effect. The other possible hypothesis could be that the cells are able to adapt quickly to DCA mediated changes in mitochondrial metabolism, while metformin mediated inhibition of Complex I is irreversible. Therefore, a better way to study DCA's long term effect would be to add fresh media with the drug everyday. Data from this study is too small to conclude the mechanism of the transient effect of DCA, however this raises an intriguing question as to how should DCA doses be monitored if it goes for clinical trial.

A small increase in lactate production after metformin treatment was seen. This is due to the blocking of Complex I of electron transport chain which stimulates glycolysis, so that the cells can compensate the ATP production and improve the bioenergetics. We also showed that direct activation of AMPK doesn't induce lactate production by using AICAR. Moreover, our result showed that lactate production by metformin needs indirect activation of AMPK by blocking complex I. However, Buzzai *et. al* [19] showed that the rate of lactate production was highly induced by metformin in AMPK<sup>+/+</sup> and p53<sup>+/+</sup> compared to AMPK<sup>-/-</sup> and p53<sup>-/-</sup> cells, indicating that AMPK is required for metformin induced glycolysis. Rotenone, a known



pharmacological inhibitor of complex I, can be used to understand the mechanism of metformin induced glycolysis and its dependence on AMPK activation.

Another novel finding of the study was activation of AMPK by DCA. Most of the studies done on DCA have focused only on DCA's activity on PDK. This study provides an insight into another potential pathway that DCA acts on which ultimately results in activation of AMPK. The *in vivo* study of DCA done by our lab showed that p53 heterozygous mice treated with DCA had lower weight than the control, indicating that DCA might have increased the fatty acid oxidation by activating AMPK which inactivates ACC by phosphorylation [39].

There are two upstream kinases phosphorylating AMPK, LKB1 and (CaMKK $\beta$ ) [24]. LKB1 phosphorylates AMPK in an AMP dependent manner, while (CaMKK $\beta$ ) pathway works independently of AMP levels [40]. Hardie *et. al* [24] suggested that LKB1 has a high basal activity and continuously phosphorylates AMPK at Thr-172, but it is immediately dephosphorylated. However, when AMP/ATP increases, AMP binds to the  $\gamma$  subunit of AMPK, causing a conformational change which inhibits the immediate dephosphorylation of AMPK after being activated by LKB1. With DCA treatment, we are decreasing the AMP/ATP ratio by increasing the ATP production in the cells (Figure 3.13). So we hypothesize that DCA activates AMPK via AMP-independent pathway by using (CaMKK $\beta$ ). DCA treatment increases the mitochondrial metabolism, which leads to the production of reactive oxygen species (ROS). Moreover, DCA has been shown to increase oxygen consumption *in vitro* in dose-dependent manner and cause a significant increase in tumor hypoxia *in vivo* within an hour of DCA i.p. injection [41]. Hypoxia and ROS is believed to activate AMPK by increasing the intracellular Ca<sup>2+</sup> and activating (CaMKK $\beta$ ) pathway leading to AMPK phosphorylation in the absence of increases in the AMP/ATP ratio [40].

To understand DCA and AMPK interaction, further studies should focus on DCA treatment on HeLa cells (as LKB1 is mutant in HeLa cells), which will help us understand if DCA is activating AMPK via LKB1 or not. Moreover, Ca<sup>2+</sup> signaling pathway should be studied to explore novel

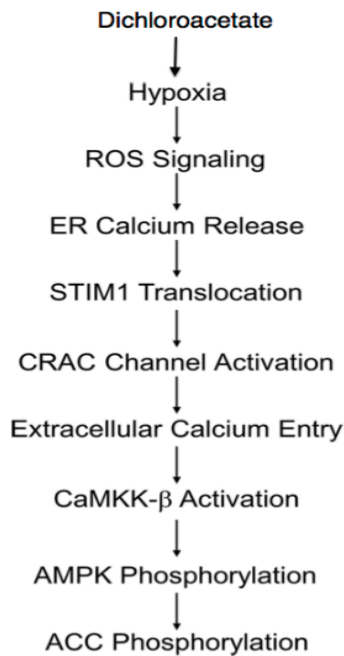


**Figure 4.1.** A model for DCA induced phosphorylation of AMPK. Dichloroacetate results in hypoxia and increased ROS production, which leads to release of  $\text{Ca}^{2+}$  from endoplasmic reticulum(ER) and translocation of STMI (a sensor of calcium stores in ER) to ER domains near the plasma membrane. STMI then activates CRAC (calcium release activated calcium) channels via direct physical interactions with the Orai subunits. This facilitates  $\text{Ca}^{2+}$  influx. Increased cytosolic  $\text{Ca}^{2+}$  activates (CaMKK $\beta$ ), which phosphorylates AMPK. Adapted from Mungai et. al, 2011.

molecular targets of DCA.

## 4.2 Robustness Analysis

It is unavoidable in any experiment that uses machine reading to have some form of measurement error. The conclusion we have reached so far that both DCA and metformin are significant alone and in combination (at 5% level) should be: a) robust to any outliers and; b) should be free of any measurement error. In the remaining of the section we follow the following steps to check the robustness of our results:

1. Using our raw neutral red assay readings, we use ordinary least squares (OLS) and robust regression to estimate the effect of DCA, metformin and DCA-metformin together on cell

proliferation. We correct for possible outliers using robust regression, which matches the median of the data and median is unaffected by any outliers.<sup>1</sup>

2. Concurrently, to control for possible measurement error while quantifying the cell viability, we use the classical measurement error model, where we postulate that if  $Y^*$  is the true reading then in our experiment we only observe  $Y$ , which is a contaminated version  $Y^*$  and the contamination is additively separable and the relationship between  $Y$  and  $Y^*$  is given by  $Y = Y^* + u$ .
3. In the next step we estimate the variance of the measurement error and subtract from the variance of the parameter. To estimate the variance we exploit the fact that we have multiple readings of the same experiment. Using only the subsample of the reading (in particular the first two readings for all the experiments) we compute the variance of the measurement error and subtract it from the variance of the parameters.
4. Then using the new “corrected” standard error we conduct a t-test to see if the estimated coefficients are statistically significantly negative.

### 4.2.1 Ordinary Least Squares

In this section we shall estimate the linear model of dependence between cell viability and DCA, metformin and DCA-metformin. Our data consists of  $\{Y_i, X_{1i}, X_{2i}\}, i = 1, \dots, N$ , where  $Y$  is the raw neutral red reading,  $X_1$  is the concentration of DCA and  $X_2$  is the concentration of metformin. Since we are interested in synergistic effect of DCA-metformin, we can create a new random variable  $X_3$  by multiplying  $X_1$  and  $X_2$ . We use the following linear model to estimate the relationship

$$Y = \beta_0 + \beta_1 X_1 + \beta_2 X_2 + \beta_3 X_3 + \epsilon, \quad (4.1)$$

---

<sup>1</sup>OLS is sensitive to outliers because it uses the mean.

variables	obs	mean	std. error	min	max
<b>nrdata</b>	825	.5	.3	.05	1.5
<b>dca</b>	825	1.6	2	0	5
<b>met</b>	825	.3	.4	0	1
<b>dcamet</b>	825	.5	1.1	0	5

**Table 4.1.** Summary Statistics

where  $\epsilon$  is the estimation error and is assumed to be Gaussian random variable with mean  $\mu_\epsilon$  and variance  $\sigma_\epsilon^2$ . In Table (4.1) we present the summary statistic of all the variables.

To estimate the parameters  $\beta$  we consider concentration of metformin only up to 1mM and use the classic projection theorem, also known as ordinary least squares estimation (OLS); for more see [42].<sup>2</sup> Given previous studies, and our previous result we expect the estimates  $(\hat{\beta}_1, \hat{\beta}_2, \hat{\beta}_3)$  to be negative and significant. Negative parameter shows that higher concentration lowers cell viability.<sup>3</sup>

The OLS result is presented in Table (4.2) and as can be seen, the parameters are all negative and significant (the reported  $p$ - values are all less than 0.05).<sup>4</sup> This shows that when we test the null  $H_0 : \hat{\beta} = 0$  against the alternative  $H_A : \hat{\beta} < 0$  we reject the null to conclude that DCA and metformin alone and in combination have significant impact on cell viability. This result agrees with the synergy seen with R index method.

variables	coefficient	std. error	t	p-value
<b>dca</b>	-0.4	0.01	-8.46	0.000
<b>met</b>	-1	0.34	-2.90	0.004
<b>dcamet</b>	-0.3	0.13	-2.11	0.036
<b>constant</b>	0.6	0.02	38.20	0.000

**Table 4.2.** Ordinary Least Squares Estimates

<sup>2</sup>We restrict the concentration of metformin because we want to stick to one of our objectives of enhancing the anti-cancer effect of metformin at a lower dose with DCA.

<sup>3</sup>All the estimations reported here were done using Stata and Matlab.

<sup>4</sup>The standard error of the coefficient is computed by finding the asymptotic distribution of the estimated parameter  $\hat{\beta}$  and as expected depends on both the variance of  $X$ 's and  $\sigma_\epsilon^2$ .

### 4.2.2 Robust Regression

We want to confirm that the previous results are not driven by outliers in the data. A simple plot of the data (not reported in here, but available upon request) confirms that we cannot confidently rule out presence of outliers. To address this problem, we use Robust Regression where we match the data to the median and not the mean like in OLS. The estimation result is presented in Table (4.3). We still find that the parameters are negative and that DCA and metformin treatments independently are significant but there is no synergy between the two. This puts a doubt on the robustness of the previous findings. As mentioned earlier this could have been driven by measurement error.

variables	coefficient	std. error	t	p-value
dca	-0.5	0.007	-6.87	0.000
met	-0.1	0.36	-2.87	0.004
dcamet	-0.02	0.14	-1.68	0.092
constant	0.7	0.02	36.52	0.000

**Table 4.3.** Robust Regression Estimates

### 4.2.3 Measurement Error

Until now we have assumed that all the relevant variables were measured without any error. In reality however, there are reasons to believe that error is introduced during laboratory analysis and sampling. In the light of this and the conclusion from the robust regression, we must control the effect of measurement error.

But before that we must verify if there is any variability in  $Y$  that cannot be explained by observed variation in the concentration. To check that we can look at the replicated experiments. In each of such replication, because the concentration of DCA and metformin are fixed the reading of  $Y$  should not vary too much from the within-experiment mean. Suppose we have four readings  $R_1, \dots, R_4$  with the same  $X$ 's then  $(R_i - \bar{R})$  should be very close to 0. As seen in (Figure 4.2) this is not the case and in fact there is a lot of variation across each replication, which provides

support that there might be some measurement error.

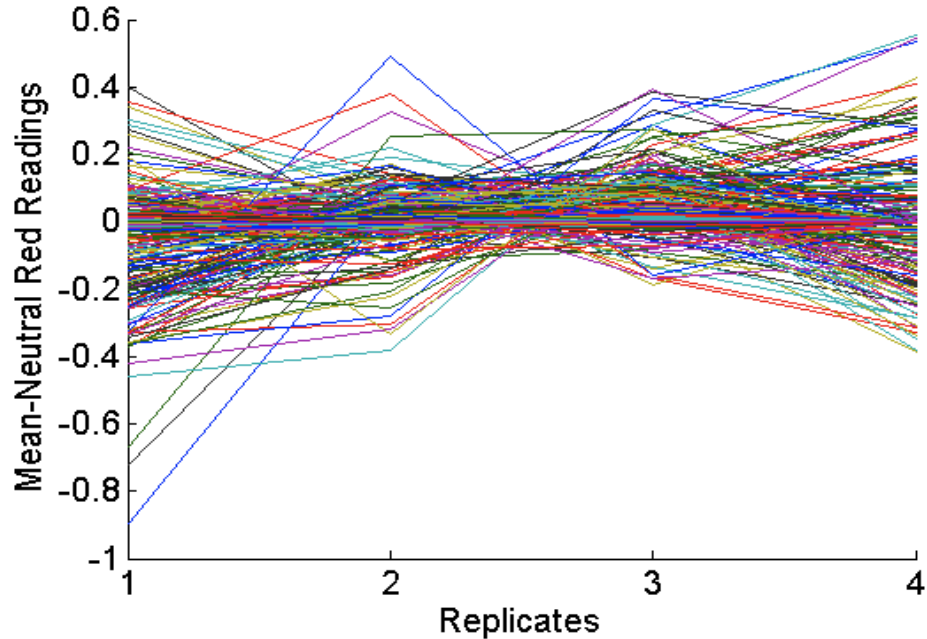


**Figure 4.2.** Variance among the four replicates of raw neutral red data.

In this experiment, we have a strong reason to believe that if any of the variables are mis-measured then it must be the neutral red reading, i.e. the random variable  $Y$ , our dependent variable. For simplicity we postulate that the error is additively separable and is Gaussian with zero mean and unknown variance. Since measurement error in the dependent variable (and not in  $X$ ) does not change the estimates of the parameter but only inflates the standard error and hence effects the test statistics, how we model the variance of the measurement error is crucial [43]. More importantly, the next question is if the measurement error is depended on the true neutral red readings. Although, given the experimental environment there is no reason to believe that the measurement error systematically depends on the true  $Y^*$  we must first find evidence against that. In (Figure 4.3) we depict the relationship between standard deviation and mean of replicates of  $Y$  and the linear robust regression (in red) shows that there is no obvious trend and hence the variability present in the experiment does not depend on our readings.

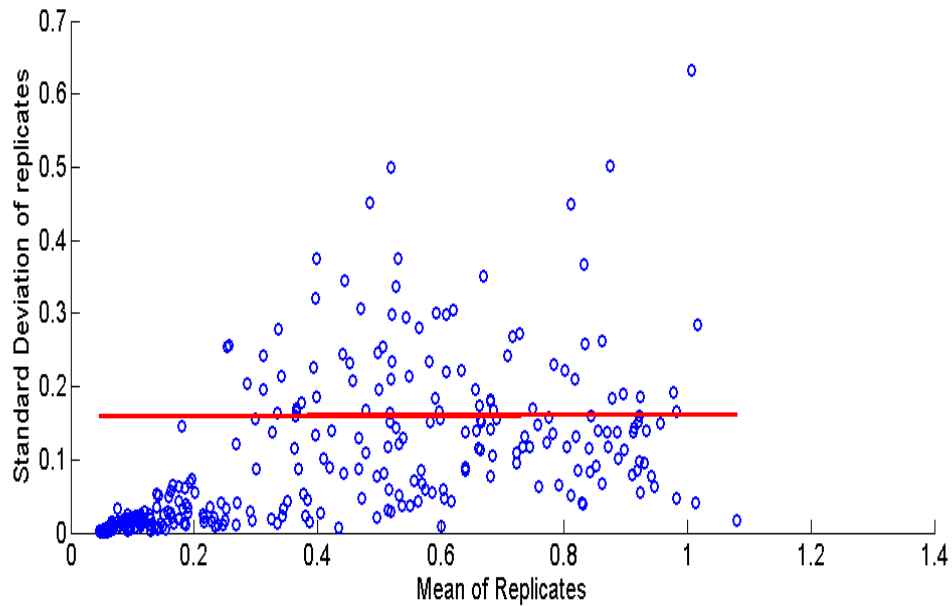


**Figure 4.3.** Standard deviation vs. the mean of replicates for raw neutral red data. Each point represents the mean and standard deviation of four replicates in each experiment. The solid line is the predicted relationship between standard deviation and mean of replicates.

This means that we can safely assume that the error has homogenous variance i.e. it is homoskedastic. Its variance is given by a fixed number  $\sigma_u^2$  [44] [45]. Let  $Y^*$  be the true neutral red reading but what the machine reads and what we measure is  $Y$  and  $Y \neq Y^*$  and

$$Y = Y^* + u; \quad u \sim N(0, \sigma_u^2). \quad (4.2)$$

So, when had we ignored measurement error, instead of using the correct model, which is

$$Y^* = \beta_0 + \beta_1 X_1 + \beta_2 X_2 + \beta_3 X_3 + \nu, \quad (4.3)$$

we were using the incorrect model given in Equation (4.1).<sup>5</sup> In other words, when we estimate

---

<sup>5</sup>Note that the correct model is infeasible because we do not observe  $Y^*$  but the incorrect model is feasible.

parameters using Equation (4.1) we were estimating

$$Y = \beta_0 + \beta_1 X_1 + \beta_2 X_2 + \beta_3 X_3 + \underbrace{\nu + u}_{=\epsilon}, \quad (4.4)$$

where  $\epsilon$  is the composite error of Equation (4.1). That is to say that the estimated standard error was inflated by the presence of  $u$ . This follows from the observation that in Equation (4.1) the estimated variance of parameters  $\hat{\beta}$  is equal to  $\frac{\sigma_\epsilon^2}{\text{Var}(X)}$  and because  $\sigma_\epsilon^2 = \sigma_\nu^2 + \sigma_u^2$ , when we computed the test statistic

$$t = \frac{\hat{\beta}}{s.e.(\beta)}$$

the absolute value would have been deflated leading us to conclude (erroneously) that the parameter was not significantly different from zero. The true test statistic should not be dependent on  $\sigma_\epsilon^2$  but depend only on  $\sigma_\nu^2$ . Therefore, the natural next step is to estimate the variance of the measurement error and subtract it from  $\sigma_\epsilon^2$  to get the variance of estimation  $\sigma_\nu^2$  and use it to compute the test statistics.<sup>6</sup>

Recall the structure of the experiment. For each pair of DCA and metformin, we have at least three and sometimes four replications. Now, to estimate the variance of measurement error (which is all we need at this stage to correct the standard error of the estimates), first we consider only two readings of  $Y^*$ . Since the right hand side variables are held fixed, the recorded reading  $Y_i$  is just a deviation from the true  $Y^*$ . To this end we consider the following model (with slightly different notations to avoid any confusion):

$$R_{1i} = Y_i^* + u_{1i}$$

---

<sup>6</sup>As alluded earlier, this measurement error does not affect the estimated value of the parameters and only its standard error. Moreover, the validity of the test also test depends on the assumption that the errors are Gaussian, at least asymptotically. We verify this later using quantile-quantile plot see (Figure 4.4).



$$R_{2i} = Y_i^* + u_{2i},$$

where  $R_1$ . and  $R_2$ . are the two replicated measurement of true  $Y^*$  and  $u_1$ . and  $u_2$ . are the respective errors. Hence,  $R_1$  and  $R_2$  measure the same  $Y^*$  but none of the variables in the RHS of the equations are observed. It would be impossible (without more information) to ascertain the values of the errors for each reading. However, as mentioned earlier we only care about the variance of  $u_i$ , whose sample analog is

$$Var(u) = \frac{\sum_{i=1}^N (R_{2i}^2 - R_{1i}R_{2i})}{N} + \frac{\sum (R_{1i}^2 - R_{1i}R_{2i})}{N}.$$

The estimate of the variance  $\hat{\sigma}_n^2 = 0.019474823$ . Then we use the remaining subsample of reading to estimate the parameters (and the variances). In Tables (4.4, 4.5) we have the estimation results for the third and the fourth neutral red readings, from where we get our variance of the  $\hat{\beta}$ . Once we subtract  $\frac{\hat{\sigma}_n^2}{X'X}$  from  $\frac{\hat{\sigma}_\beta^2 + \hat{\sigma}_n^2}{X'X}$  we get the adjusted variance of the  $\hat{\beta}$ . But before we use the t-test we want to also make sure that our assumption of Gaussian distribution of measurement error cannot be invalidated by the data.<sup>7</sup> In view of the scope of this research, we use a visual method, based on Quantile-Quantile plot, to ascertain if we can reject normality of the errors. The idea is very intuitive: Once we estimate the parameters of the model (either OLS or robust regression) we can estimate the errors by subtracting the predicted  $Y$  from the observed  $Y$ . Then, we can fit in a density through the estimated errors and randomly draw quantiles from the estimated density. We can then compare those quantiles with the quantiles that are drawn from Gaussian density. If the quantiles are from the same densities, i.e. Gaussian, then the two should align themselves along a 45-degree line. If not, then we can be sure that the estimated errors are not Gaussian. This result is shown in (Figure 4.4) from which we can safely conclude that the

---

<sup>7</sup>The assumption of Gaussian distribution is also important for the asymptotic distribution of the test statistic.

variables	coefficient	std. error	t	P
dca1	-.03	.01	-3.30	0.001
met1	-.13	.05	-2.67	0.01
dcamet1	-.03	.02	-1.74	0.083
constant	.68	.02	27.87	0.000

**Table 4.4.** Estimated parameters for reading 3 and reading 4 from OLS

Gaussian assumption is not completely erroneous.<sup>8</sup>

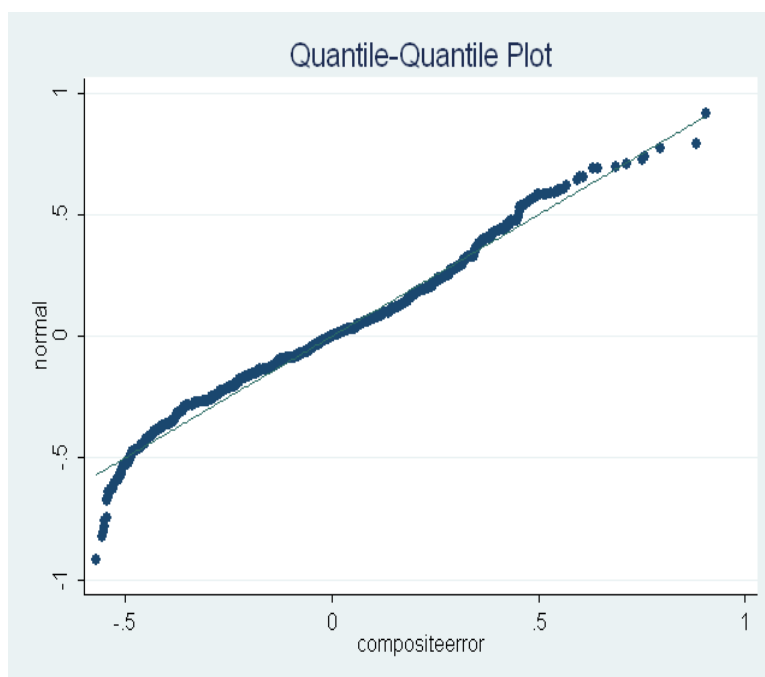


**Figure 4.4.** Q-Q plot of composite error and a theoretical normal distribution. The fact that quantiles of the two distributions align along a 45° line indicate that the estimated errors are Gaussian.

Now that we have confirmed validity of the classical measurement error assumption, we can be confident about our model. For completeness we present the results for both OLS and robust regression Table(4.6) and thereby conclude that the effect of DCA and metformin both inhibit the growth and most importantly they have synergy between the two, which is also statistically significant.

<sup>8</sup>We use Stata to compute and plot the quantiles.

variables	coefficient	std. error	t	P
dca1	-.04	.01	-3.49	0.001
met1	-.13	.05	-2.58	0.010
dcamet1	-.03	.02	-1.58	0.115
constant	.69	.03	26.67	0.000

**Table 4.5.** Estimated parameters for reading 3 and reading 4 from robust regression

Ordinary Least Square Estimator				Robust Regression Estimator		
Variables	std. error	t	P	std. error	t	P
DCA	< 0.001	-51.9	< 0.0001	< 0.001	-48.2	<0.0001
metformin	0.003	-41.8	< 0.0001	0.003	-38.9	<0.0001
DCA*metformin	0.001	-28.2	< 0.0001	0.001	-26.1	<0.0001

**Table 4.6.** Corrected estimates for OLS and robust regression

### 4.3 Conclusions

The study showed that DCA and metformin work together on reducing the cell proliferation but have counter effects on inducing ATP and lactate production. The synergistic effect seen in this study is robust to measurement error. However, the effect seen isn't enough to conclude that the interaction between two compounds will be useful for cancer treatment as this study was limited to a single cell line -V14 derived from mice. Therefore, further work must be done in human breast cancer cell lines to validate the results. In this study we also demonstrated that DCA can activate AMPK. Inhibition of PDK is unlikely to induce the activation of AMPK by DCA. Therefore we propose that there are other molecular targets of DCA that are still unexplored.

# Bibliography

- [1] SIEGEL, R., E. WARD, O. BRAWLEY, and A. JEMAL (2011) “Cancer statistics, 2011,” *CA: A Cancer Journal for Clinicians*, **61**(4), pp. 212–236.  
URL <http://dx.doi.org/10.3322/caac.20121>
- [2] HANAHAHAN, D. and R. A. WEINBERG (2000) “The Hallmarks of Cancer,” *Cell*, **100**(1), pp. 57–70.  
URL [http://dx.doi.org/10.1016/S0092-8674\(00\)81683-9](http://dx.doi.org/10.1016/S0092-8674(00)81683-9)
- [3] ——— (2011) “Hallmarks of Cancer: The Next Generation,” *Cell*, **144**(5), pp. 646–674.
- [4] PATEL, M. S. and L. G. KOROTCHKINA (2003) “The biochemistry of the pyruvate dehydrogenase complex\*,” *Biochemistry and Molecular Biology Education*, **31**(1), pp. 5–15.  
URL <http://dx.doi.org/10.1002/bmb.2003.494031010156>
- [5] BONNET, S., S. L. ARCHER, J. ALLALUNIS-TURNER, A. HAROMY, C. BEAULIEU, R. THOMPSON, C. T. LEE, G. D. LOPASCHUK, L. PUTTAGUNTA, S. BONNET, G. HARRY, K. HASHIMOTO, C. J. PORTER, M. A. ANDRADE, B. THEBAUD, and E. D. MICHELAKIS (2007) “A Mitochondria-K<sup>+</sup> Channel Axis Is Suppressed in Cancer and Its Normalization Promotes Apoptosis and Inhibits Cancer Growth,” *Cancer Cell*, **11**(1), pp. 37 – 51.
- [6] WARBURG, O. (1956) “On the Origin of Cancer Cells,” *Science*, **123**(3191), pp. 309–314.
- [7] MICHELAKIS, E. D., L. WEBSTER, and J. R. MACKEY (2008) “Dichloroacetate (DCA) as a potential metabolic-targeting therapy for cancer,” *Br J Cancer*, **99**(7), pp. 989–994.
- [8] CAIRNS, R. A., I. S. HARRIS, and T. W. MAK (2011) “Regulation of cancer cell metabolism,” *Nat Rev Cancer*, **11**(2), pp. 85–95.  
URL <http://dx.doi.org/10.1038/nrc2981>
- [9] GATENBY, R. A. and R. J. GILLIES (2004) “Why do cancers have high aerobic glycolysis?” *Nat Rev Cancer*, **4**(11), pp. 891–899.  
URL <http://dx.doi.org/10.1038/nrc1478>
- [10] STACPOOLE, P. W., N. V. NAGARAJA, and A. D. HUTSON (2003) “Efficacy of Dichloroacetate as a Lactate-Lowering Drug,” *The Journal of Clinical Pharmacology*, **43**(7), pp. 683–691, <http://jcp.sagepub.com/content/43/7/683.full.pdf+html>.  
URL <http://jcp.sagepub.com/content/43/7/683.abstract>
- [11] SUN, R., M. FADIA, J. DAHLSTROM, C. PARISH, P. BOARD, and A. BLACKBURN (2010) “Reversal of the glycolytic phenotype by dichloroacetate inhibits metastatic breast cancer

- cell growth in vitro and in vivo,” *Breast Cancer Research and Treatment*, **120**, pp. 253–260, 10.1007/s10549-009-0435-9.
- [12] CRABB, D. W., E. A. YOUNT, and R. A. HARRIS (1981) “The metabolic effects of dichloroacetate,” *Metabolism*, **30**(10), pp. 1024 – 1039.  
URL <http://www.sciencedirect.com/science/article/pii/0026049581901050>
- [13] STACPOOLE, P. W., L. R. GILBERT, R. E. NEIBERGER, P. R. CARNEY, E. VALENSTEIN, D. W. THERIAQUE, and J. J. SHUSTER (2008) “Evaluation of Long-term Treatment of Children With Congenital Lactic Acidosis With Dichloroacetate,” *Pediatrics*, **121**(5), pp. e1223–e1228.
- [14] STACPOOLE, P. W., D. S. KERR, C. BARNES, S. T. BUNCH, P. R. CARNEY, E. M. FENNELL, N. M. FELITSYN, R. L. GILMORE, M. GREER, G. N. HENDERSON, A. D. HUTSON, R. E. NEIBERGER, R. G. O’BIEN, L. A. PERKINS, R. G. QUISLING, A. L. SHROADS, J. J. SHUSTER, J. H. SILVERSTEIN, D. W. THERIAQUE, and E. VALENSTEIN (2006) “Controlled Clinical Trial of Dichloroacetate for Treatment of Congenital Lactic Acidosis in Children,” *Pediatrics*, **117**(5), pp. 1519–1531.
- [15] EVANS, J. M. M., L. A. DONNELLY, A. M. EMSLIE-SMITH, D. R. ALESSI, and A. D. MORRIS (2005) “Metformin and reduced risk of cancer in diabetic patients,” *BMJ*, **330**(7503), pp. 1304–1305.
- [16] LI, D., S.-C. J. YEUNG, M. M. HASSAN, M. KONOPLEVA, and J. L. ABBRUZZESE (2009) “Antidiabetic Therapies Affect Risk of Pancreatic Cancer,” *Gastroenterology*, **137**(2), pp. 482 – 488.  
URL <http://www.sciencedirect.com/science/article/pii/S0016508509005551>
- [17] WRIGHT, J. and J. STANFORD (2009) “Metformin use and prostate cancer in Caucasian men: results from a population-based case–control study,” *Cancer Causes and Control*, **20**, pp. 1617–1622, 10.1007/s10552-009-9407-y.  
URL <http://dx.doi.org/10.1007/s10552-009-9407-y>
- [18] PHOENIX, K., F. VUMBACA, and K. CLAFFEY (2009) “Therapeutic metformin/AMPK activation promotes the angiogenic phenotype in the ER negative MDA-MB-435 breast cancer model,” *Breast Cancer Research and Treatment*, **113**, pp. 101–111, 10.1007/s10549-008-9916-5.  
URL <http://dx.doi.org/10.1007/s10549-008-9916-5>
- [19] BUZZAI, M., R. G. JONES, R. K. AMARAVADI, J. J. LUM, R. J. DEBERARDINIS, F. ZHAO, B. VIOLLET, and C. B. THOMPSON (2007) “Systemic Treatment with the Antidiabetic Drug Metformin Selectively Impairs p53-Deficient Tumor Cell Growth,” *Cancer Research*, **67**(14), pp. 6745–6752, <http://cancerres.aacrjournals.org/content/67/14/6745.full.pdf+html>.  
URL <http://cancerres.aacrjournals.org/content/67/14/6745.abstract>
- [20] BEN SAHRA, I., C. REGAZZETTI, G. ROBERT, K. LAURENT, Y. LE MARCHAND-BRUSTEL, P. AUBERGER, J.-F. TANTI, S. GIORGETTI-PERALDI, and F. BOST (2011) “Metformin, independent of AMPK, induces mTOR inhibition and cell cycle arrest through REDD1,” *Cancer Research*, **71**(13), pp. 4366–4372.
- [21] JIRALERSPONG, S., S. L. PALLA, S. H. GIORDANO, F. MERIC-BERNSTAM, C. LIEDTKE, C. M. BARNETT, L. HSU, M.-C. HUNG, G. N. HORTOBAGYI, and A. M. GONZALEZ-ANGULO (2009) “Metformin and Pathologic Complete Responses to Neoadjuvant Chemotherapy in Diabetic Patients With Breast Cancer,” *Journal of Clinical Oncology*,

- 27**(20), pp. 3297–3302, <http://jco.ascopubs.org/content/27/20/3297.full.pdf+html>.  
URL <http://jco.ascopubs.org/content/27/20/3297.abstract>
- [22] LIU, B., Z. FAN, S. M. EDGERTON, X.-S. DENG, I. N. ALIMOVA, S. E. LIND, and A. D. THOR (2009) “Metformin induces unique biological and molecular responses in triple negative breast cancer cells,” *Cell Cycle*, **8**(13), pp. 2031–2040.  
URL <http://www.landesbioscience.com/journals/cc/article/8814/>
- [23] SHAW, R. J., K. A. LAMIA, D. VASQUEZ, S.-H. KOO, N. BARDEESY, R. A. DEPINHO, M. MONTMINY, and L. C. CANTLEY (2005) “The Kinase LKB1 Mediates Glucose Homeostasis in Liver and Therapeutic Effects of Metformin,” *Science*, **310**(5754), pp. 1642–1646, <http://www.sciencemag.org/content/310/5754/1642.full.pdf>.  
URL <http://www.sciencemag.org/content/310/5754/1642.abstract>
- [24] HARDIE, D. G. (2011) “Sensing of energy and nutrients by AMP-activated protein kinase,” *The American Journal of Clinical Nutrition*, **93**(4), pp. 891S–896S, <http://www.ajcn.org/content/93/4/891S.full.pdf+html>.  
URL <http://www.ajcn.org/content/93/4/891S.abstract>
- [25] KUDCHODKAR, S. B., G. Q. DEL PRETE, T. G. MAGUIRE, and J. C. ALWINE (2007) “AMPK-Mediated Inhibition of mTOR Kinase Is Circumvented during Immediate-Early Times of Human Cytomegalovirus Infection,” *Journal of Virology*, **81**(7), pp. 3649–3651.
- [26] INOKI, K., T. ZHU, and K.-L. GUAN (2003) “TSC2 Mediates Cellular Energy Response to Control Cell Growth and Survival,” *Cell*, **115**(5), pp. 577 – 590.  
URL <http://www.sciencedirect.com/science/article/pii/S0092867403009292>
- [27] HADAD, S. M., S. FLEMING, and A. M. THOMPSON (2008) “Targeting AMPK: A new therapeutic opportunity in breast cancer,” *Critical Reviews in Oncology/Hematology*, **67**(1), pp. 1 – 7.  
URL <http://www.sciencedirect.com/science/article/pii/S104084280800019X>
- [28] SHAW, R. J., N. BARDEESY, B. D. MANNING, L. LOPEZ, M. KOSMATKA, R. A. DEPINHO, and L. C. CANTLEY (2004) “The LKB1 tumor suppressor negatively regulates mTOR signaling,” *Cancer Cell*, **6**(1), pp. 91 – 99.  
URL <http://www.sciencedirect.com/science/article/pii/S1535610804001771>
- [29] ZHUANG, Y. and W. MISKIMINS (2008) “Cell cycle arrest in Metformin treated breast cancer cells involves activation of AMPK, downregulation of cyclin D1, and requires p27<sup>Kip1</sup> or p21<sup>Cip1</sup>,” *Journal of Molecular Signaling*, **3**, pp. 1–11, 10.1186/1750-2187-3-18.  
URL <http://dx.doi.org/10.1186/1750-2187-3-18>
- [30] SAHRA, I. B., K. LAURENT, A. LOUBAT, S. GIORGETTI-PERALDI, P. COLOSETTI, P. AUBERGER, J. F. TANTI, Y. LE MARCHAND-BRUSTEL, and F. BOST (2008) “The antidiabetic drug metformin exerts an antitumoral effect in vitro and in vivo through a decrease of cyclin D1 level,” *Oncogene*, **27**(25), pp. 3576–3586.  
URL <http://dx.doi.org/10.1038/sj.onc.1211024>
- [31] EL-MIR, M.-Y., V. NOGUEIRA, E. FONTAINE, N. AVÉRET, M. RIGOLET, and X. LEVERVE (2000) “Dimethylbiguanide Inhibits Cell Respiration via an Indirect Effect Targeted on the Respiratory Chain Complex I,” *Journal of Biological Chemistry*, **275**(1), pp. 223–228, <http://www.jbc.org/content/275/1/223.full.pdf+html>.  
URL <http://www.jbc.org/content/275/1/223.abstract>

- [32] BATANDIER, C., B. GUIGAS, D. DETAILLE, M. EL-MIR, E. FONTAINE, M. RIGOLET, and X. LEVERVE (2006) "The ROS Production Induced by a Reverse-Electron Flux at Respiratory-Chain Complex 1 is Hampered by Metformin," *Journal of Bioenergetics and Biomembranes*, **38**, pp. 33–42, 10.1007/s10863-006-9003-8.  
URL <http://dx.doi.org/10.1007/s10863-006-9003-8>
- [33] BLACKBURN, A. C., S. C. McLARY, R. NAEEM, J. LUSZCZ, D. W. STOCKTON, L. A. DONEHOWER, M. MOHAMMED, J. B. MAILHES, T. SOFERR, S. P. NABER, C. N. OTIS, and D. J. JERRY (2004) "Loss of Heterozygosity Occurs via Mitotic Recombination in Trp53+ Mice and Associates with Mammary Tumor Susceptibility of the BALB/c Strain," *Cancer Research*, **64**(15), pp. 5140–5147, <http://cancerres.aacrjournals.org/content/64/15/5140.full.pdf+html>.  
URL <http://cancerres.aacrjournals.org/content/64/15/5140.abstract>
- [34] VALDIVIESO-GARCIA, A., R. CLARKE, K. RAHN, A. DURETTE, D. MACLEOD, and C. GYLES (1993) "Neutral red assay for measurement of quantitative vero cell cytotoxicity," *Applied and Environmental Microbiology*, **59**(6), pp. 1981–1983.
- [35] KERN, D. H., C. R. MORGAN, and S. U. HILDEBRAND-ZANKI (1988) "In Vitro Pharmacodynamics of 1--d-Arabinofuranosylcytosine: Synergy of Antitumor Activity with cis-Diamminedichloroplatinum(II)," *Cancer Research*, **48**(1), pp. 117–121, <http://cancerres.aacrjournals.org/content/48/1/117.full.pdf+html>.  
URL <http://cancerres.aacrjournals.org/content/48/1/117.abstract>
- [36] ROMANELLI, S., P. PEREGO, G. PRATESI, N. CARENINI, M. TORTORETO, and F. ZUNINO (1998) "In vitro and in vivo interaction between cisplatin and topotecan in ovarian carcinoma systems," *Cancer Chemotherapy and Pharmacology*, **41**, pp. 385–390, 10.1007/s002800050755.  
URL <http://dx.doi.org/10.1007/s002800050755>
- [37] BEUTLER, E. (1975) *Red Cell Metabolism. A Manual of Biochemical Methods*, 2 ed., Grune and Stratton, New York.
- [38] WONG, J. Y., G. S. HUGGINS, M. DEBIDDA, N. C. MUNSHI, and I. D. VIVO (2008) "Dichloroacetate induces apoptosis in endometrial cancer cells," *Gynecologic Oncology*, **109**(3), pp. 394 – 402.  
URL <http://www.sciencedirect.com/science/article/pii/S009082580800098X>
- [39] MINOKOSHI, Y., Y.-B. KIM, O. D. PERONI, L. G. D. FRYER, C. MULLER, D. CARLING, and B. B. KAHN (2002) "Leptin stimulates fatty-acid oxidation by activating AMP-activated protein kinase," *Nature*, **415**(6869), pp. 339–343.  
URL <http://dx.doi.org/10.1038/415339a>
- [40] MUNGAI, P. T., G. B. WAYPA, A. JAIRAMAN, M. PRAKRIYA, D. DOKIC, M. K. BALL, and P. T. SCHUMACKER (2011) "Hypoxia Triggers AMPK Activation through Reactive Oxygen Species-Mediated Activation of Calcium Release-Activated Calcium Channels," *Molecular and Cellular Biology*, **31**(17), pp. 3531–3545, <http://mcb.asm.org/content/31/17/3531.full.pdf+html>.  
URL <http://mcb.asm.org/content/31/17/3531.abstract>
- [41] CAIRNS, R. A., K. L. BENNEWITH, E. E. GRAVES, A. J. GIACCIA, D. T. CHANG, and N. C. DENKO (2009) "Pharmacologically Increased Tumor Hypoxia Can Be Measured by 18F-Fluoroazomycin Arabinoside Positron Emission Tomography and Enhances Tumor Response to Hypoxic Cytotoxin PR-104," *Clinical Cancer Research*, **15**(23), pp. 7170–7174,

<http://clincancerres.aacrjournals.org/content/15/23/7170.full.pdf+html>.  
URL <http://clincancerres.aacrjournals.org/content/15/23/7170.abstract>

- [42] LUENBERGER, D. G. (1969) *Optimization by Vector Space Method*, Wiley.
- [43] FULLER, W. A. (1987) *Measurement Error Models*, Wiley.
- [44] LIPSITZ, S. R. (1992) "Methods for Estimating the Parameters of a Linear Model for Ordered Categorical Data," *Biometrics*, **48**(1), pp. pp. 271–281.  
URL <http://www.jstor.org/stable/2532755>
- [45] RAO, C. (2002) *Linear Statistical Inference and Its Applications*, second ed., Wiley.



## Academic Vita

### Samagya Banskota

10 Vairo Boulevard, State College, PA 16803  
Email: syb5109@psu.edu, samagya.banskota@anu.edu.au

#### EDUCATION

The Pennsylvania State University, University Park, USA (August, 2008-May, 2012)  
Schreyer Honors College  
Bachelor of Science  
Honors in Bioengineering with Mechanical Engineering Option

#### AFFILIATION

Visiting Scholar (August, 2011-Present)  
The John Curtin School of Medical Research  
The Australian National University, Canberra, Australia

#### RESEARCH EXPERIENCES

The Australian National University, Canberra, Australia  
Cancer Metabolism & Therapy Lab

**Visiting Scholar (Honors Research)** (August, 2011-Present)

##### Research Topic

- Re-engineering breast cancer metabolism using metformin and dichloroacetate

Fox Chase Cancer Center, Philadelphia, USA

Dr. Andrew Godwins Lab

**Undergraduate Research Fellow** (June-August, 2010)

##### Research Topic

- Proteomic biomarkers for breast cancer detection

The Pennsylvania State University, University Park, USA

Cellular Biomechanics Lab

**Research Assistant** (October, 2009-November, 2010)

##### Research Topic

- Local velocity profile around tumor cells adhered to endothelial cells in the presence of neutrophils (PMN) in flow using micro-PIV and side-view image technique

#### PAST ACADEMIC PROJECTS

- Fabrication of weighing scale under \$10 for Mashavu Telemedicine Venture in Kenya
- Portable, at-home Electroencephalograph (EEG) fabrication
- Designed artificial cornea using Bacterial Cellulose/Polyvinyl Alcohol

#### AWARDS

- The Presidents Freshman Award 2009
- 2009-10 Anita M. Todd Internship Student of the Year
- Deans List Penn State University (for all enrolled semesters)
- Schreyer's International Thesis Research Grant 2011
- Summer Fellowship at Fox Chase Cancer Center (Summer 2010)